Electronic Supplementary Material (ESI) for Nanoscale.

Supporting Information

β-1,3-glucan synthesis, novel supramolecular self-assembly, characterization and application

Robert Pylkkänen, Pezhman Mohammadi, Ville Liljeström, Wojciech Płaziński, Grégory Beaune, Jaakko Timonen, and Merja Penttilä

Table of Contents

Experimental Procedures

Materials

Glucose was bought from Anapur. α-D-Glucose 1-phosphate (G7000), acetaminophen, acetylsalicylic acid and HEPES were bought from Sigma-Aldrich.

Cloning, expression and purification of Ta1,3BGP

The nucleotide sequence of the β-1,3-glucan phosphorylase gene (*bgp*) from *Thermosipho africanum* was synthesized by Eurofins Genomics (Espoo, Finland) in codon-optimized form for expression in yeast *Saccharomyces cerevisiae*. The *bgp* gene was cloned into a yeast expression vector under regulation of the constitutive *ENO1* promoter and *ENO1* terminator using yeast homologous recombination. The resulting plasmid, (pRPC-041) contained the *URA3* selection marker and the 2-micron origin of replication for autonomous replication in yeast. For protein purification, a 6×His-tag was included in the N-terminal end of the *bgp* gene. Plasmids were transformed into *Escherichia coli* XL1-Blue cells for replication, and the correct plasmid was confirmed with sequencing and transformed into the *S. cerevisiae* Inv*Sc*1 strain (genotype: *MATa*, *his3Δ1*, *leu2*, *trp1-289*, *ura3-52*/*MATα*, *his3Δ1*, *leu2*, *trp1-289*, and *ura3-52*) using the lithium acetate method.[1] Transformants were selected for uracil prototrophy on SCD^{-URA} (20 g/L glucose and 6.7 g/L yeast nitrogen base, supplemented with appropriate amino acids).

For protein expression, the resulting strain yRP-260 was grown in 500 mL of SCD^{-URA} medium in 2.5 L Erlenmeyer flasks (for a total volume of 3 L) at 30 °C, 200 rpm. Cells were harvested by centrifugation at 2700 × *g* for 15 min and were resuspended in 50 mL of ice-cold lysis buffer (50 mM Tris-HCL, 500 mM NaCl, pH 7.4), supplemented with protease inhibitors (1 × cOmplete, EDTA-free Protease Inhibitor Cocktail, Roche). Lysis was performed with three passes through a French press at 10.000 psi, and the cells were cooled on ice between the passes.

For protein purification, the cell lysate was centrifuged at 27,000 × *g* for 45 minutes at 4 °C, and the supernatant was loaded on a 5 mL HiTrap Chelating HP column equilibrated with 50 mM Tris-HCl and 500 mM NaCl, pH 7.4. *Ta*1,3BGP was eluted with a 30 mL gradient from 0 to 500 mL imidazole, and fractions containing *Ta*1,3BGP (analyzed by SDS-PAGE) were pooled and concentrated using Vivaspin 20, 10 kDa MWCO PES ultrafiltration device (GE Healthcare). During the concentration, the buffer was exchanged to 200 mM HEPES-NaOH, pH 7.0 with 1 mM DTT. Protein concentation was estimated with Bio-Rad Protein Assay using manufacturers standard procedure for microtiter plates.

β-1,3-glucan synthesis

All enzymatic reactions were carried out in 200 mM HEPES-NaOH buffer, pH 7.0 with 1 mM DTT. The employed glycosyl donor (α-D-glucose 1-phosphate) and glycosyl acceptor (glucose) concentrations were kept at 200, and 50 mM, respectively. The concentration of *Ta*1,3BGP was kept at 260 nM, and the reactions were started by the addition of enzyme. After the reactions were carried out, the insoluble fractions were separated by centrifugation and washed three times in DDIW.

Phosphate Release

Release of inorganic phosphate from α-D-glucose 1-phosphate was measured using the Malachite Green Phosphate Assay Kit (POMG-25H, BioAssay Systems). Briefly, 20 µL of malachite green reagent was mixed with 80 µL of reaction supernatant (diluted 1:5000 in DDIW) in a 96-well plate. The plate was incubated at room temperature for 45 minutes, and released phosphate was quantified by measuring absorbance at 620 nm and comparing against a standard inorganic phosphate curve according to manufacturer's protocol. Standard deviations were calculated from the average of three replicates, and the curve_fit function of SciPy module was used to fit the mean of the three replicates to Gompertz sigmoid curve function

$$f(t) = a\exp(-\exp^{b-ct}) \quad (1)$$

where *t* corresponds to time, *a* is an asymptote, *b* sets the displacement along time-axis, and *c* sets the growth rate.

Size-Exclusion Chromatography (SEC)

Insoluble reaction products were separated by centrifugation, washed three times in DDIW, freeze-dried, and dissolved in 1 M NaOH. Relative molar masses were determined using size-exclusion chromatography in 0.1 M NaOH eluent. The differential molar mass distributions were calculated against pullulan standards (Shodex, Germany).

To estimate the height, center and standard deviation for the three observed molar mass distribution peaks, the curve_fit (non-linear least squares) function of SciPy module was employed to fit the sum of three Gaussian functions

$$f(x) = \sum a_n \exp\left(-\frac{(x-\mu_n)^2}{2{\sigma_n}^2}\right) \quad (2)$$

where *x* is the slice log molecular weight, a_n is the is height of peak n, μ_n is the position of the center of peak n, and σ_n is the standard deviation of peak n. The average molar masses ($\bar{M}_n$, $\bar{M}_w$) were then calculated for each peak according to the formulas

$$\bar{M}_n = \frac{\sum N_i M_i}{\sum N_i} \quad (3)$$

$$\bar{M}_w = \frac{\sum N_i M_i^2}{\sum N_i M_i} \quad (4)$$

where the summation is over all the molecular weights and N_i is the number of molecules with weight M_i, with values obtained from the previously fitted Gaussian function for each peak.

Matrix-assisted Laser Desorption/Ionization Time-of-Flight Mass Spectrometry (MALDI-ToF-MS)

MALDI-ToF-MS was performed as described elsewhere.[2] Briefly, reactions were carried out in 1 mL Eppendorf tubes in heatblocks with temperatures measured 4, 25, 37, 42, 50, 65, and 80 °C. After the insoluble fractions were separated by centrifugation and washed three times in DDIW, they were freeze-dried and resuspended at DDIW at 2.5 mg/mL concentration. 0.5 µL of the aqueous suspensions were directly spotted on a MALDI target and mixed with 1 µL of 10 mg/mL 2,5-dihydroxybenzoic acid in 50 % acetonitrile-0.1 % (v/v) trifluoroacetic acid. MALDI-ToF spectra were recorded on an ultrafleXtreme III MALDI-ToF/ToF instrument (Bruker Daltonics, Germany) and calibrated using Peptide Calibration Standard II (Bruker Daltonics, Germany).

For data processing, baseline was subtracted using the ZhangFit[3] (adaptive iteratively reweighted penalized least squares) function of BaselineRemoval Python module, after which all intensity values were normalized between mean and 1.0. Peaks with peak height greater than standard deviation were located using with a peak-to-peak mass difference greater than 161.9 Da were identified using find_peaks function of scipy.signal module, and peak widths with peak_widths function of scipy.signal module. Average molar masses ($\overline{M}_n$, $\overline{M}_w$) were calculated according to equations (2, 3), where N_i corresponds to area between the ith peak and mean (0), and M_i corresponds the molar mass of that species.[2]

Scanning Electron Microscopy (SEM)

Reactions were carried out in 1 mL Eppendorf tubes in heatblocks with temperatures measured at 4, 25, 37, 42, 50, 65, and 80 °C. After the insoluble fractions were separated and washed, they were resuspended in 1 mL DDIW and 3 µL of the aqueous solutions was plunged into a mixture of propane and ethane (-180 °C) to preserve internal structures. Samples were then handled under liquid nitrogen and transferred into a FreeZone 4.5 L Cascade Benchtop Freeze DrySystems freeze-drier equipped with a collection chamber at -105 °C.

Imaging was performed with a Zeiss FE-SEM field emission microscope with variable pressures operating at 1 - 1.5 kV. A thin platinum coating was sputtered onto sample surface prior to imaging. Image processing was done in ImageJ (version 1.53e).

Optical and confocal microscopy

After reactions were carried out in 1 mL Eppendorf tubes in heatblocks with temperatures measured 4, 25, 37, 42, 50, 65, and 80 °C, the insoluble fractions were separated by centrifugation and washed three times in DDIW after which the samples were resuspended in 1 mL DDIW. Confocal microscope (LSM 710, 40x/1.1 water-immersion and 63x/1.4 DIC oil-immersion objectives) was used to image the produced insoluble particles and was operated at in transmission mode (λex = 458 nm and λem = 463 – 735 nm). Images were exported from the instrument software (Zeiss Zen Black) in CZI format and further processed using Matplotlib and Numpy packages in Python.

In order to follow β-1,3-glucan synthesis *in situ* using an optical microscope, the reactions were carried out in sealed glass capillary tubes 0.10 mm x 2.00 mm x 5 cm with synthesis temperature being kept at 50 °C. Temperature was controlled using a thermostate (RE420, controlhead ECO GOLD, Lauda) coupled to cooling/heating incubation insert (P-Set 20000, TempController 2002-2, PeCon) for the microscope stage, in which the capillary was placed.

All optical microscope imaging was done using an inverted microscope (Nikon Eclipse Ti) with a 60x/0.95 DIC objective and associated with a 1.5x magnification device. Movies of the particles inside the capillaries were recorded using a CCD camera (Andor Zyla Scmos) with a time interval of 0.5 s.

Micropipette aspiration

Micropipettes with diameters of 25 µm and 10 µm were prepared by pulling borosilicate capillaries (WPI, 1 mm, 0.58 mm OD/ID) with a magnetic puller (PN-31, Narishige), and then callibrating and bending them with a microforge (MF-900, Narishige). The micropipettes were connected to a water reservoir attached to a piezoelectric pressure controller unit (Elveflow) and filled with water. Aspiration was performed by increasing pressure by 100 mbar intervals from 0 to 1 bar using the instrument software. Imaging was done using the optical microscope described above with a 20x/0.45 objective associated with a 1.5x magnification device.

Small-angle X-ray scattering (SAXS)

SAXS data was obtained using a Xenocs Xeuss 3.0 SAXS/WAXS system (Xenocs SAS, Grenoble, France). The system includes a microfocus X-ray source (sealed tube) with a Cu target and a multilayer mirror which yields a parallel beam with a nominal wavelength of 1.542 Å (combined Cu K-α1 and Cu K-α2 characteristic radiation). The source operates at 50 kV and 0.6 mA. The

beam is collimated by a set of variable slits and the beam size at the sample was 0.7 mm during the experiment. The system does not include a beam stop, which enables direct measurement of sample transmission. The data was acquired using an area detector (Eiger2 R 1M, Dectris AG, Switzerland) that was in the evacuated chamber. The sample-to-detector distance was calibrated by measuring the diffraction from a known LaB6 standard sample.

β-1,3-glucan synthesis was carried out in a glass capillary tube as described for optical microscopy. Mark-tubes made of borosilicate glass with an outer diameter of 1.5 mm and wall thickness of 10 µm were attached to the heating block using silicon paste. The reaction temperature was set to constant 50 °C, controlled by Instec mK2000B temperature controller connected to a Instec LN2-PBU (Instec, Inc. USA) liquid nitrogen pump. The Instec setup uses resistive heating and liquid nitrogen cooling for temperature control. The reagents were mixed in the Mark-tube and the tubes were sealed by hot glue.

SAXS data measurements were started 28 minutes after the synthesis reactions were started and continued by collecting 1-minute frames for a total of 120 measurements. The final measurement was performed 196 minutes after the reaction was started. As the first 5 measurements did not show any scattering from aggregated structures (flat scattering profile), these scattering profiles were averaged and treated as the background scattering, which was subtracted from all following measurements.

In SAXS experiments the scattering intensity is proportional to both the nanoscale electron density contrast and the mass of material in the interaction volume (X-ray beam). Importantly, the mass of aggregated sediment settled in the X-ray beam was variable and unknown during the experiment. Consequently, the information optimally obtained from the magnitude of the scattering intensity is uncertain, and from the SAXS analysis we do not make any conclusion regarding electron density of the aggregates.

For model fitting, the data was split into 30 sections each consisting of 4 measurements for which the measured intensity was averaged. A paracrystal lamellar model was employed for model fitting.[4] Briefly, the formula for correlating scattering intensity *I(q)* with the scattering vector *q* is calculated as

$$I(q) = 2\pi\Delta\rho_m{}^2\Gamma_m \frac{P_{bil}(q)}{q^2} Z_N(q) \qquad (5)$$

where $\Delta\rho_m$ is the difference in scattering length per unit mass of solute between particles and solvent and Γ_m is the mass per area of bilayer. P_{bil}, the form factor of the bilayer is approximated as the cross section of an infinite, planar bilayer of thickness t

$$P_{bil}(q) = \left(\frac{\sin(qt/2)}{qt/2}\right)^2 \qquad (6)$$

and $Z_N(q)$ describes the interference effects for aggregates consisting of more than one bilayer

$$Z_N(q) = \frac{1 - w^2}{1 + w^2 - 2w\cos(\mathrm{q}\langle D\rangle)} + x_N S_N + (1 - x_N) S_{N+1} \qquad (7)$$

where $\langle D\rangle$ is the average distance between two adjacent layers and where

$$S_N(q) = \frac{a_N}{N}[1 + w^2 - 2w\cos(q\langle D\rangle)]^2 \qquad (8)$$

and

$$a_N = 4w^2 - 2(w^3 + w)\cos(q\langle D\rangle) - 4w^{N+2}\cos(Nq\langle D\rangle) + 2w^{N+3}\cos[(N-1)q\langle D\rangle] + 2w^{N+1}\cos[(N+1)q\langle D\rangle] \qquad (9)$$

for the layer spacing distribution w

$$w = \exp(-\sigma_D^2 q^2/2) \qquad (10)$$

Finally, the calculated $I(q)$ was multiplied by a scaling parameter and a constant background was added. The data was weighted by the square root of I(q) in the fitting process to emphasize lower q values. Finally, the data was fitted to the model using curve fit function of the SciPy package. Boundary values for the relevant parameters for model optimization were set as t_{min} = 50 Å, t_{max} = 100 Å, N_{min} = 50, N_{max} = 200, $\langle D\rangle_{min}$ = 100 Å, $\langle D\rangle_{max}$ = 200 Å.

Wide-angle X-ray scattering (WAXS)

Reactions were carried out in 50 mL Falcon tubes in ovens with temperatures set to 4, 25, 37, 42, 50, 65, and 80 °C. After three days, the insoluble fractions were separated by centrifugation, washed three times in DDIW and freeze-dried. WAXS was carried out using a Bruker D8 equipped with scintillation counter detectors. The collection was performed using CuKα radiation with λ = 1.5418 Å (energy of 40 kV and 40 mA). The diffractometer collected at 2θ range of 10 - 60 ° with a step size of 0.01 °/second and 1.5 second exposure time per-step and scanning time of 2 hours per sample with the scan-type locked couple (reflection mode). Synchrotron measurements were carried out at the µSpot beamline at BESSY II synchrotron (Berliner Elektronenspeicherring-Gesellschaft für

Synchrotronstrahlung, Helmholtz-Zentrum Berlin, Germany) equipped with Eiger X 9M detector with a pixel size of 75×75 µm. The energy exposure was 15 keV (0.82656 Å) using a silicon 111 monochromator and a beam size of 100 µm. Samples were sealed in thin-walled boron-rich capillary tubes. For data processing, baseline was substracted by using the ZhangFit[3] (adaptive iteratively reweighted penalized least squares) function of BaselineRemoval Python module.

Drug release measurements

β-1,3-glucan synthesis was carried out in 50 mL Falcon tubes in an oven set to 50 °C for a total volume of 300 mL. In order to quantify the concentration of the produced glucan, 5 mL aliquots were freeze-dried overnight in 5 mL Eppendorf tubes and the weight of dry β-1,3-glucan was determined gravimetrically. 5 mg/mL stocks of acetaminophen and acetylsalicylic acid were prepared in 50 mL Falcon tubes, and amounts corresponding to 80 mg β-1,3-glucan and 1 mL of DDIW, acetaminophen or acetylsalicylic acid stocks were mixed with β-1,3-glucan overnight at 100 rpm after which the samples were freeze-dried overnight. The resulting powders were pressed into tablets using a ... tablet press, and drug release was quantified by resuspending the tablets in phosphate buffer, pH 7.0 and quantifying the amounts of acetaminophen and acetylsalicylic acid in the supernatant by measuring absorbances at 312 and 330 nm respectively. For data processing, the curve_fit function of SciPy module was used to fit M_t, the cumulative amount of drug released at time t, according to the Weibull function[5]

$$M_t = M_\infty[1 - \exp(-at^b)] \qquad (11)$$

where a and b are constants and M_∞ corresponds to the cumulative amount of drug released at infinite time.

Mechanical testing

Tablets prepared as described in drug release measurements were subjected to fracture support RIG test. Measurements were performed using TA.XTExpressC Texture Analyser stable micro system equipped with 100 N load cell using a flat face cylindrical probe with a diameter of 5 mm moving down (2.5 µm/sec) onto the disks centrally positioned over circular support, up to the point of fracture failure. Recorded data were processed and analyzed using the combination of originLAB version 2019 and Exponent Connect software.

Computational methods

The atomistic molecular dynamics (MD) simulations concerned the following systems: (1) a single triple helix (TH) composed of the three β-1,3-glucan chains of length of 26 residues; (2,3) the two complexes composed of the associated two THs, arranged either in parallel or antiparallel direction; (4) a periodic, quasi-infinite layer composed of 16 TMs, packed according to hexagonal symmetry and parallel mutual arrangement; (5) the two fragments of layers mentioned in point (4), each containing 19 THs and exhibiting hexagonal symmetry with respect to either TH packing and limiting edges; (6) a set of non-associated 16 THs, uniformly distributed across simulation box according to square symmetry and maintaining mutual parallel arrangement. The initial geometry of a single TH (point (1)) was based on the crystal structure deposited in the polysac3db.cermav.cnrs.fr database and prepared by using the GROMACS[6] in-built tool *editconf*. The remaining initial structures from points (2)-(6) were built basing on the fully equilibrated structure of a single TH.

The GROMOS 56a6$_{CARBO/CARBO_R}$ force field[7] was used to describe the interactions within the system in all MD simulations along with simple point charge (SPC), GROMOS-compatible water model, accounting for the presence of explicit water[8]. All MD simulations were carried out with the GROMACS 2016.4 package[6].

The studied molecules were placed in cubic or triclinic simulation boxes of dimension dependent on the system type and surrounded by the number of explicit water molecules approximately accounting for the solvent density of 1 g/cm^3. The detailed compositions of the systems are given in Tab. S1 The MD simulations were carried out under periodic boundary conditions and in the isothermal-isobaric ensemble. The temperature was maintained close to its reference value (323 K) by applying the V-rescale thermostat[9] (two separate coupling groups, i.e. β-1,3-glucan and water), whereas for the constant pressure (1 bar, semiisotropic coordinate scaling for system (4), isotropic scaling for remaining systems) the Parrinello-Rahman barostat[10] was used with a relaxation time of 0.4 ps. The equations of motion were integrated with a time step of 2 fs using the leap-frog scheme[11]. The translational center-of-mass motion was removed every timestep separately for the solute and the solvent. The full rigidity of the water molecules was enforced by application of the SETTLE procedure[12]. The solute bond lengths were constrained by application of the LINCS procedure with a relative geometric tolerance of 10^{-4}.[13] The non-bonded interactions were calculated using a single cutoff distance set to 1.4 nm and Verlet list scheme. The reaction-field correction was applied to account for the mean effect of the electrostatic interactions beyond the long-range cut off distance, using a relative dielectric permittivity of 61 as appropriate for the SPC water model.[14]

In the case of systems containing ≤ 2 THs, the equilibration stage included applying weak (force constant equal to 5 kJ/mol/nm^2), harmonic distance restraints on the ring atoms of each of the two neighboring, non-covalently bound residues in the TH complex. This was necessary to avoid the spontaneous dissociation of the three β-1,3-glucan chains, being a result of minor inaccuracy of the force field. In the case of larger systems (single layer or fragments of two layers), no constraints were applied. After equilibration, MD production simulations were carried out for a duration of 200 ns (systems (1)-(4)), 500 ns (system 5)) or 114 ns (system (6)), and the data (atomic coordinates) were saved every 2 ps or 20 ps (only system (6)). Some of the simulations were triplicated in order to check the reproducibility of the results.

In addition to unbiased MD simulations, some enhanced-sampling simulations were performed for systems mentioned in points (2,3) and (4) in order to estimate the energetic characteristics of TH-TH interactions.

In the case of two interacting THs, the umbrella sampling (US) simulations were carried out. The US approach obtains the free-energy profile along a predefined 1D coordinate from a set of equilibrated simulations. The applied reaction coordinate was the distance between two THs. The pull code in GROMACS was used to generate from an initial pulling trajectory snapshots for the US simulations. Initially associated THs were pulled away with a harmonic force constant of 5000 kJ mol^{-1} nm^{-2} and a pull rate of 0.001 nm ps^{-1}. Along the reaction coordinate, 58 windows were selected in the range 1.35-4.25 nm with a distance of ~0.05 nm between the interhelical distances in adjacent US windows. In the next step the US sampling was performed by running simulations with harmonic force constant of 5000 kJ mol^{-1} nm^{-2} applied to constraint the interhelical distance and additional, harmonic bias (50 kJ mol^{-1} nm^{-2}) preventing the relative rotation of helices and spurious interactions of the end-to-edge type. The data within each window were collected every 0.1 ps (30 ns of simulation per 1 US window). The free energy profiles were constructed with the weighted histogram analysis method (WHAM)[15] as implemented in GROMACS (*wham*).[16] Statistical uncertainties were estimated using the Bayesian bootstrapping of complete histograms. The convergence of profiles was also tested by producing the profiles corresponding to the different ranges of sampling times.

In the case of hexagonal layer composed of THs (system (4)), the free energy change associated with removing a single TH from equilibrated layer was estimated by using the thermodynamic integration (TI) approach.[17] In order to complete the thermodynamic cycle, the same part of the system (i.e. a single TH) was removed from either the single layer or from the aqueous solution. This was achieved by scaling all corresponding nonbonded interactions down to zero in a stepwise manner as a function of a coupling parameter λ. The associated free energy changes were calculated with the Bennett Acceptance Ratio (BAR) method[18], implemented in the GROMACS *bar* subroutine, including the error estimation determined by using the default criteria. The 21 evenly spaced λ-points were accepted and the data from equilibrated systems were collected every 0.1 ps for a duration of either 20 ns in each λ window. The initial configuration for each λ_i window was generated from the snapshot of the λ_{i-1} simulation, after 1 ns of simulation, while configuration for λ = 0 was taken from final frames of corresponding, unbiased MD simulations. The Coulomb and van der Waals parameters were perturbed simultaneously and a soft-core function was used for the van der Waals interactions to prevent energy singularities. The final value of the free energy needed to remove single TH from fully associated layer was calculated as the difference between the free energy changes calculated either for associated layer or for single TH in solution.

The water and electron densities across the simulation box were calculated for system (5) by using the GROMACS subroutine *density*. The atomic numbers for GROMOS aliphatic (united) carbon atoms were corrected by accounting for the corresponding number of implicit hydrogen atoms.

For system (6) the simulated annealing protocol was applied. The temperature in each of the coupled groups was linearly increased from 323 to 623 K within 2 ns, then maintained at constant level of 623 K for a duration of 8 ns and, finally, decreased to 323 K within further 2 ns and maintained at this level for next 2 ns. This multistep procedure was repeated 8 times.

Table S1. The composition of the simulation systems considered in present work.

No.	Description	Initial box dimension [nm^3]	β-1,3-glucan chains	Water molecules
1	Single triple helix (TH)	9.4 × 9.4 × 9.4	3	26100
2	Parallel complex of two THs	9.4 × 9.4 × 9.4	6	25700
3	Antiparallel complex of two THs	9.4 × 9.4 × 9.4	6	25700
4	Single, periodic layer of THs	6.3 × 5.4 × 12.8*	48	6300
5	Two fragments of layer composed of THs	9.5 × 9.5 × 20	114	41200
6	Disconnected THs	10 × 10 × 10	48	25600

*triclinic box

General conformational characteristics of studied systems

System 1. A single triple helix composed of the three β-1,3-glucan chains is stable for a duration of 200 ns of unbiased MD simulation. Its thermodynamic stability can be traced back to the energetically favorable stacking of the aliphatic patches on the glucopyranose rings, supported by the lack of axial hydroxyl groups, being a potential steric hindrance. Additionally, numerous hydrogen bonding within the formed helix (ca. 64 per timeframe) support the structural stability. Contrary to the crystal structure, there exists a helical twist along the longest helix axis, equal to ca. -46 deg per one helix turn. The end-to-end distance is, on average, equal to ca. 7.5 nm and differs from the maximal value by ca. 1 nm due to internal flexibility of the whole helix and its possible bending along the longest dimension (**Fig. S22**).

Systems 2 and 3. Both parallel and antiparallel helix-helix pairing are associated with high flexibility of the resulting complex. The structure of both complexes does not exhibit a perfect, edge-to-edge alignment but there exists a distortion which manifests itself as a twist of a double-helix complex. The large number of helix-helix hydrogen bonding (ca. 21-27 per timeframe) suggest that this type of interaction may be the driving force for helix association. The main structural parameters (end-to-end distance and helical twist within single helix) remain weakly affected by the presence of another, associated helix. Moreover, these two systems were subjected to umbrella sampling-based calculations of free energy (description of the results is given below).

System 4. The MD simulation of this system allowed to determine the main structural parameters characteristic for the layer composed of aligned, hexagonally-packed triple helices. The distance between nearest neighboring helices within the layer is equal to 1.56 nm whereas the end-to-end distance for one helix (equivalent to the layer thickness) is equal to 8.74 nm. The latter value is notably larger in comparison to either single helix or helix-helix complexes due to a linear geometry of any helix enclosed in a layer, which is enforced by the close presence of neighboring helices. The layer stability is supported by the numerous hydrogen bonding between neighboring helices (ca. 37 hydrogen bonds between one neighboring pair of helices). The altered geometry of helices influences the average value of helical twist which is reduced to ca. -37 deg. Finally, it is worth mentioning that due to a high packing of helices within a layer, the whole structure is impenetrable for water. This system was subjected to thermodynamic integration protocol (description of the results is given in main manuscript).

System 5. The unbiased MD simulations demonstrated that of the two fragments of layers may undergo further complexation, forming multiple layers. However, basing on qualitative observations of the MD trajectory, this type of association is not as favorable as the edge-to-edge one, exhibited by triple helices. Moreover, the region of contact between two layers always contains non-negligible amount of water molecules, as shown in **Fig. 3h** (main manuscript).

System 6. The unbiased MD simulations with variable temperature (simulated annealing MD simulations) allowed to observe a spontaneous formation of a hexagonal structure composed of seven triple helices and of geometry analogous to a small fragment of the fully-packed layer composed of triple helices. The graphical illustration of the results is given in **Fig. S23**.

Supporting Figures

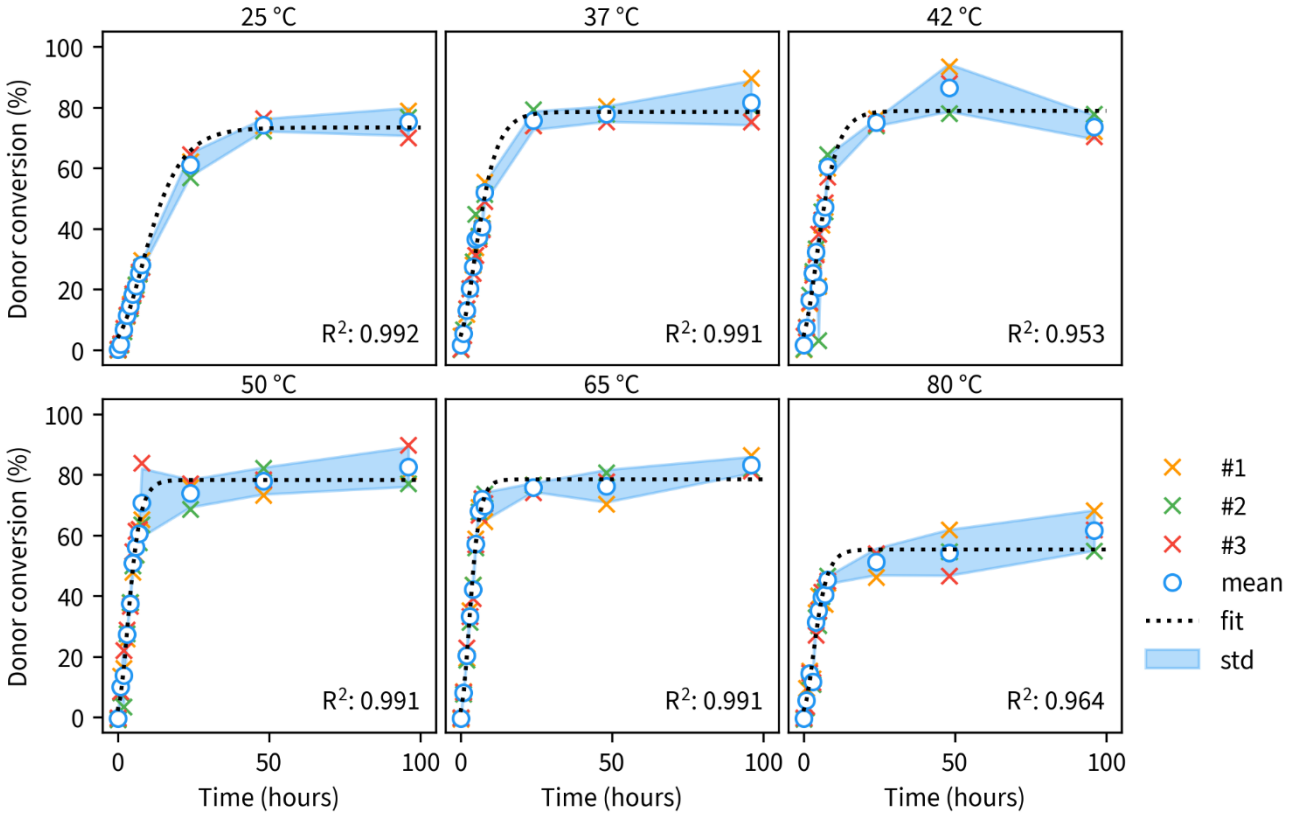

Figure S1. Phosphate release measured for the β-1,3-glucan synthesis performed at different reaction temperatures, with the corresponding temperature being indicated at the top of each panel. Three replicate measurements are visualized as blue, yellow, and green crosses, while the obtained mean values corresponding to the three replicates are shown as red circles. Area between mean and standard deviation is indicated as light blue fill. Fit obtained using Gompertz exponential function is shown as black dots and the corresponding r^2 value is indicated in the bottom right of each panel.

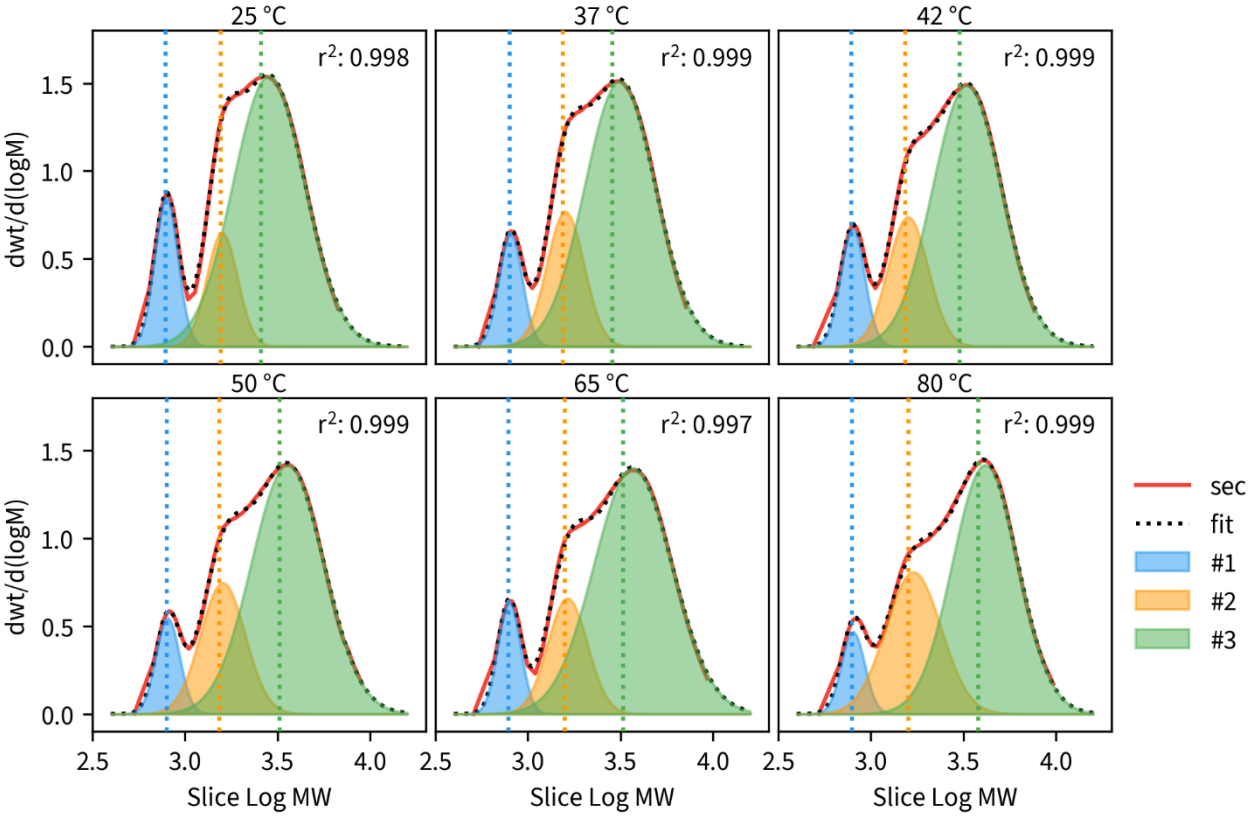

Figure S2. Size-exclusion chromatography based molar mass distributions for the insoluble β-1,3-glucans produced at different reaction temperatures, with the corresponding temperature being indicated at the top of each panel. Data obtained from the instrument is presented as a red line, and the corresponding cumulative fit obtained using equation (2) is shown as a dotted black line, with the r^2 value for the cumulative fit shown in the top right corner of each panel. Individual peak fits are filled in blue, orange, and green color in order of increasing peak average molar mass. The number average molar mass, $\bar{M}_n$, obtained from the fitted data using equation (3) is shown as a dotted vertical line corresponding to the previously assigned color for the peak.

Table S2. Molar mass distribution and fit results for β-1,3-glucan synthesized at 25, 37 and 42 °C.

	25 °C			37 °C			42 °C		
	$\bar{M}_n$	$\bar{M}_w$	PDI	$\bar{M}_n$	$\bar{M}_w$	PDI	$\bar{M}_n$	$\bar{M}_w$	PDI
Cumulative SEC	1839	2560	1.39	1992	2760	1.39	1998	2860	1.43
Cumulative Fit	1853	2623	1.42	2007	2843	1.42	2008	2921	1.45
Peak 1	783	799	1.02	796	813	1.02	786	804	1.02
Peak 2	1554	1613	1.04	1548	1635	1.06	1538	1637	1.06
Peak 3	2568	3132	1.22	2852	3457	1.21	3013	3625	1.20

Table S3. Molar mass distribution and fit results for β-1,3-glucan synthesized at 50, 65 and 80 °C.

	50 °C			65 °C			80 °C		
	$\bar{M}_n$	$\bar{M}_w$	PDI	$\bar{M}_n$	$\bar{M}_w$	PDI	$\bar{M}_n$	$\bar{M}_w$	PDI
Cumulative SEC	2134	3135	1.47	2175	3287	1.51	2244	3393	1.51
Cumulative Fit	2137	3171	1.48	2192	3384	1.54	2245	341	1.52
Peak 1	797	814	1.02	783	799	1.02	786	809	1.02
Peak 2	1537	1660	1.08	1585	1684	1.06	1538	1799	1.13
Peak 3	3234	3959	1.22	3273	4134	1.26	3013	4491	1.18

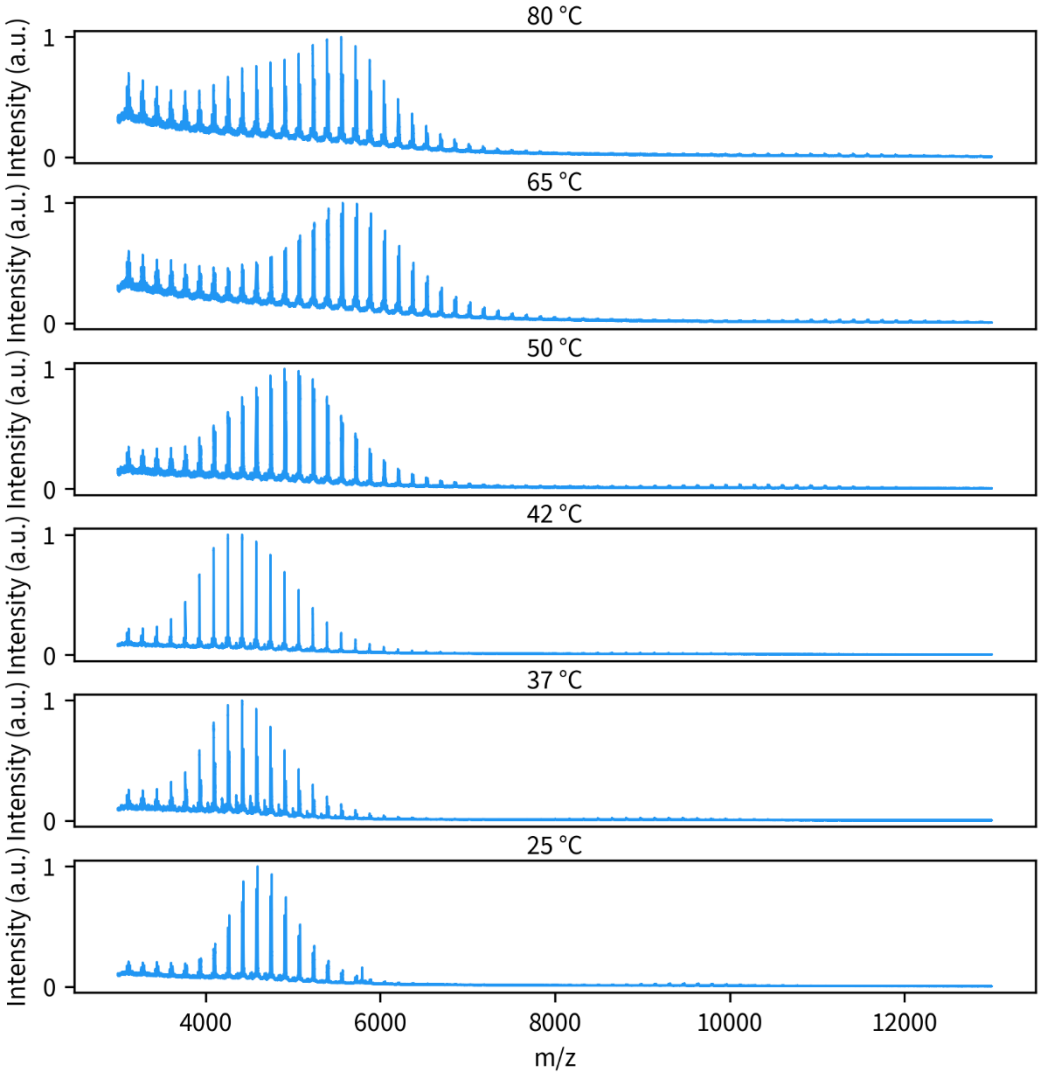

Figure S3. MALDI-ToF-MS results without background subtraction for the insoluble β-1,3-glucans produced at different reaction temperatures, with the corresponding temperature being indicated at the top of each panel.

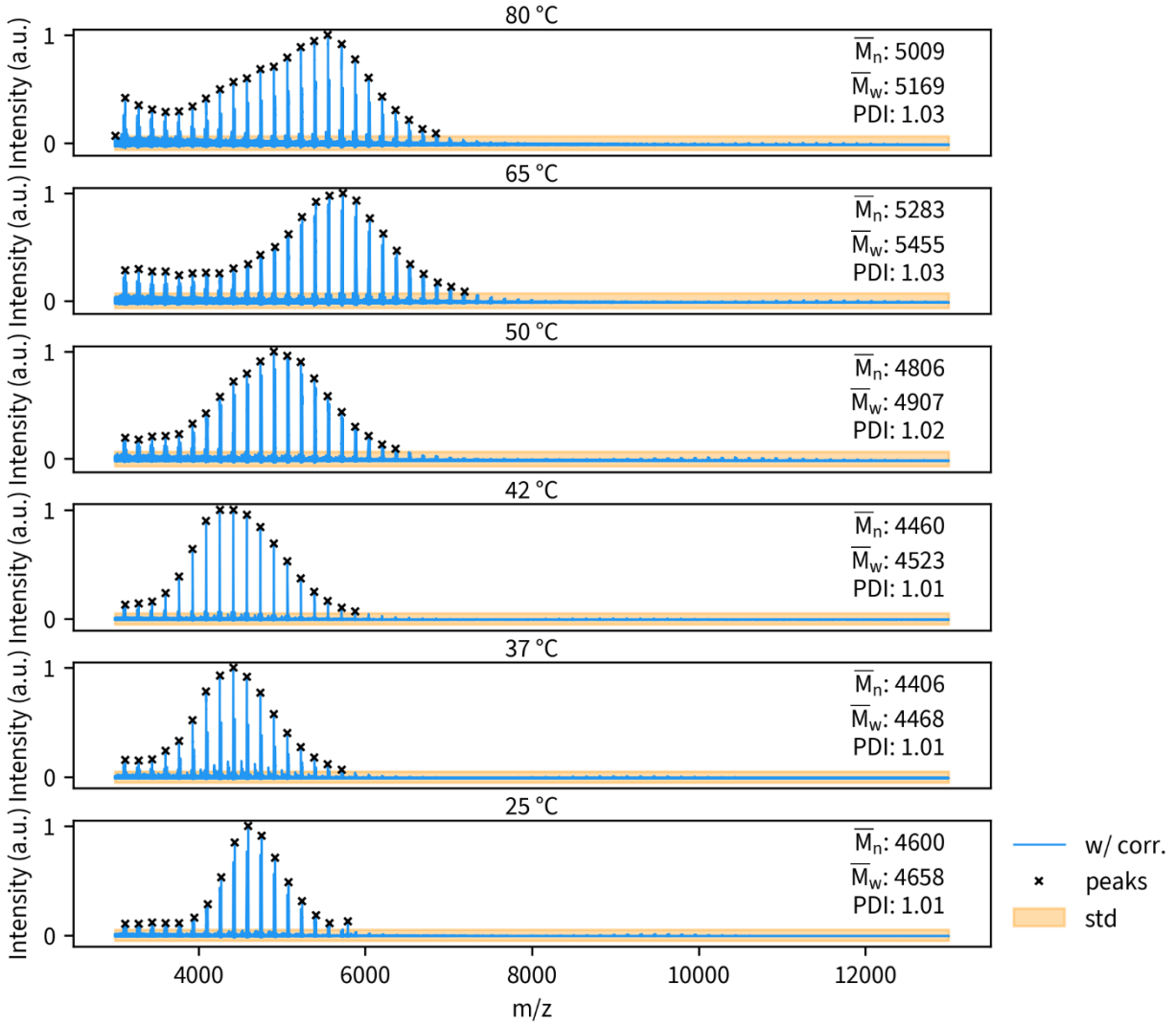

Figure S4. Processed MALDI-ToF-MS results for the insoluble β-1,3-glucans produced at different reaction temperatures, with the corresponding temperature being indicated at the top of each panel. Baseline corrected data is represented as a blue line, identified peaks with a peak-to-peak mass difference of at least 161.9 Da are shown as black crosses, standard deviation for the whole measured data is indicated as a light orange fill around the mean line. Calculated values for $\overline{M}_n$, $\overline{M}_w$, and PDI are shown in top right corner of each panel.

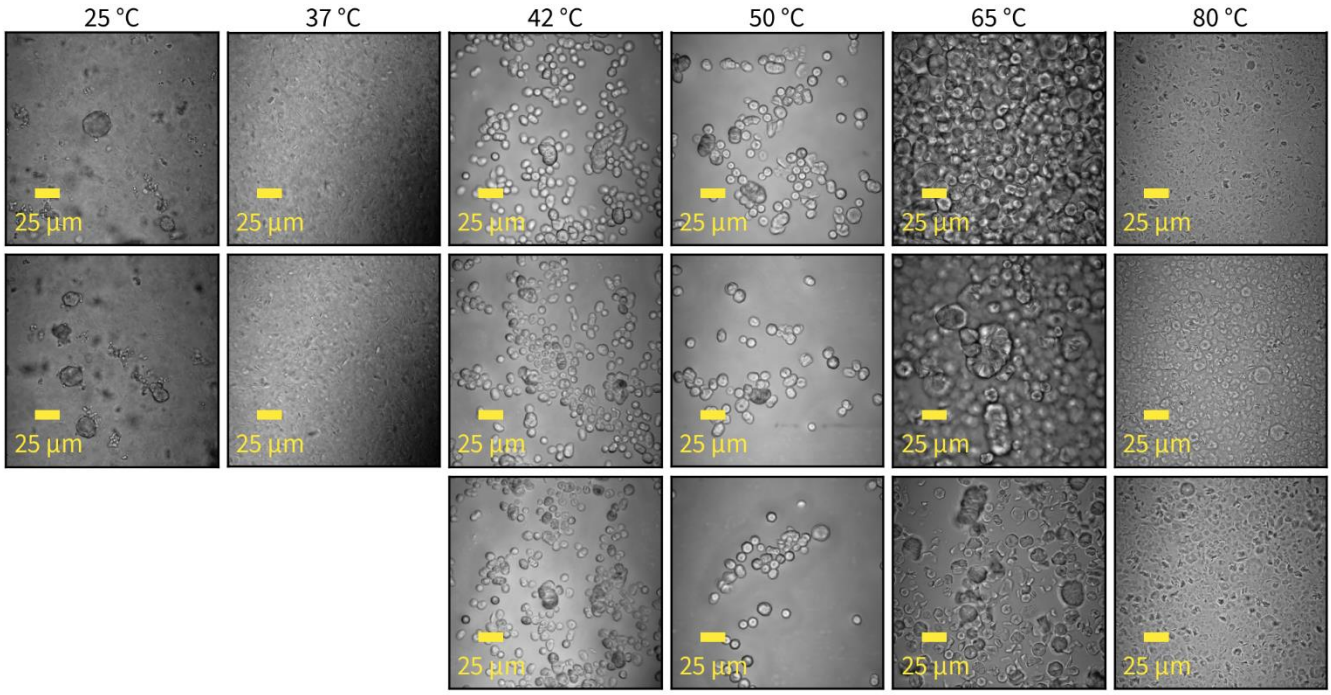

Figure S5. Confocal microscopy images of insoluble β-1,3-glucan particles synthesized at different reaction temperatures. All images were taken at the same 40x magnification, scale bar is shown in yellow in lower right corner.

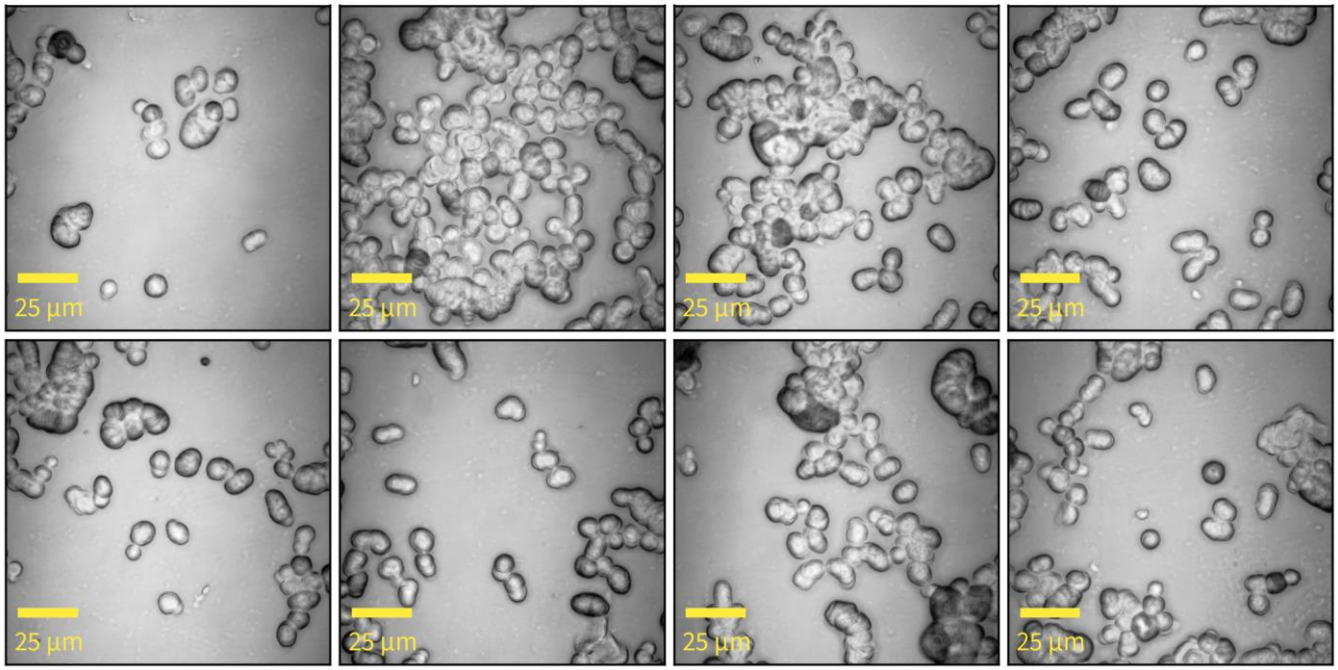

Figure S6. Confocal microscopy images of insoluble β-1,3-glucan particles synthesized at 42 °C. All images were taken at the same 63x magnification, scale bar is shown in yellow in lower left corner.

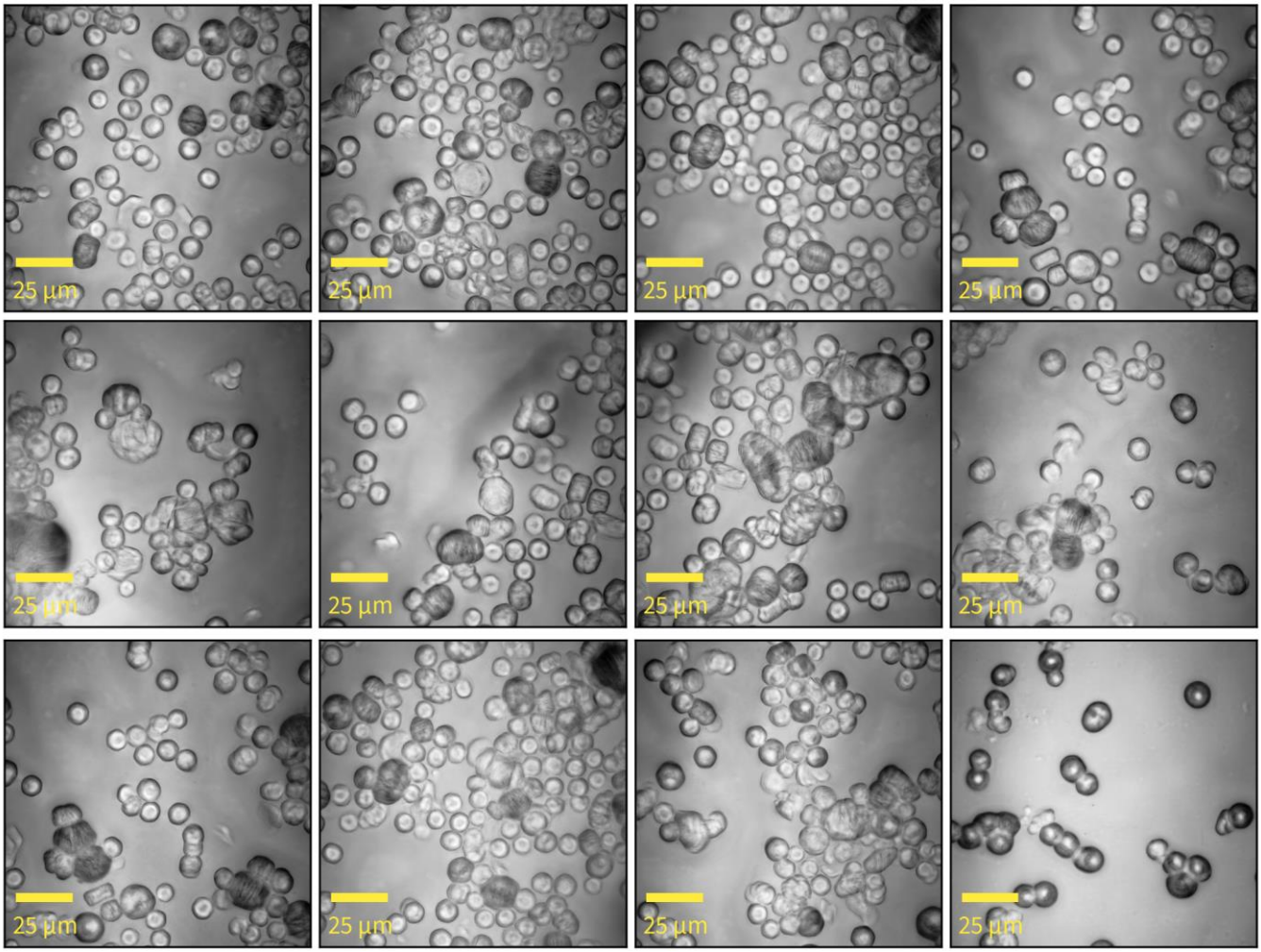

Figure S7. Confocal microscopy images of insoluble β-1,3-glucan particles synthesized at 50 °C. All images were taken at the same 63x magnification, scale bar is shown in yellow in bottom left corner.

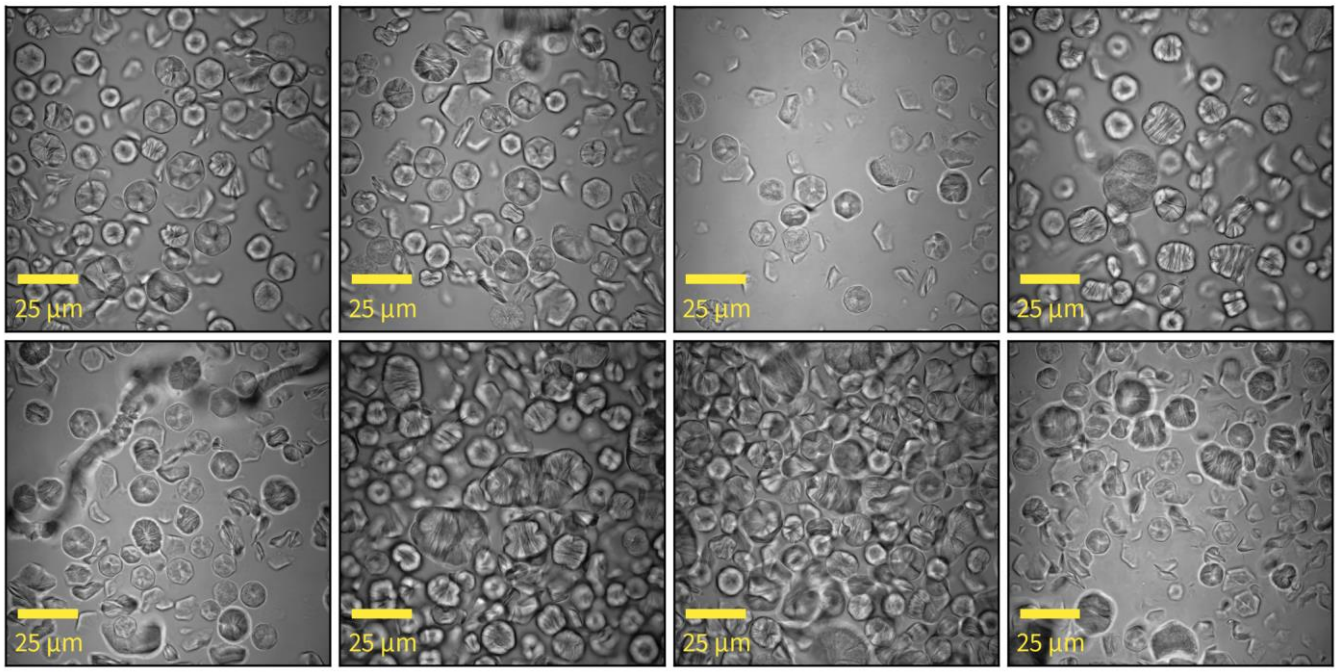

Figure S8. Confocal microscopy images of insoluble β-1,3-glucan particles synthesized at 65 °C. All images were taken at the same 63x magnification, scale bar is shown in yellow in bottom left corner.

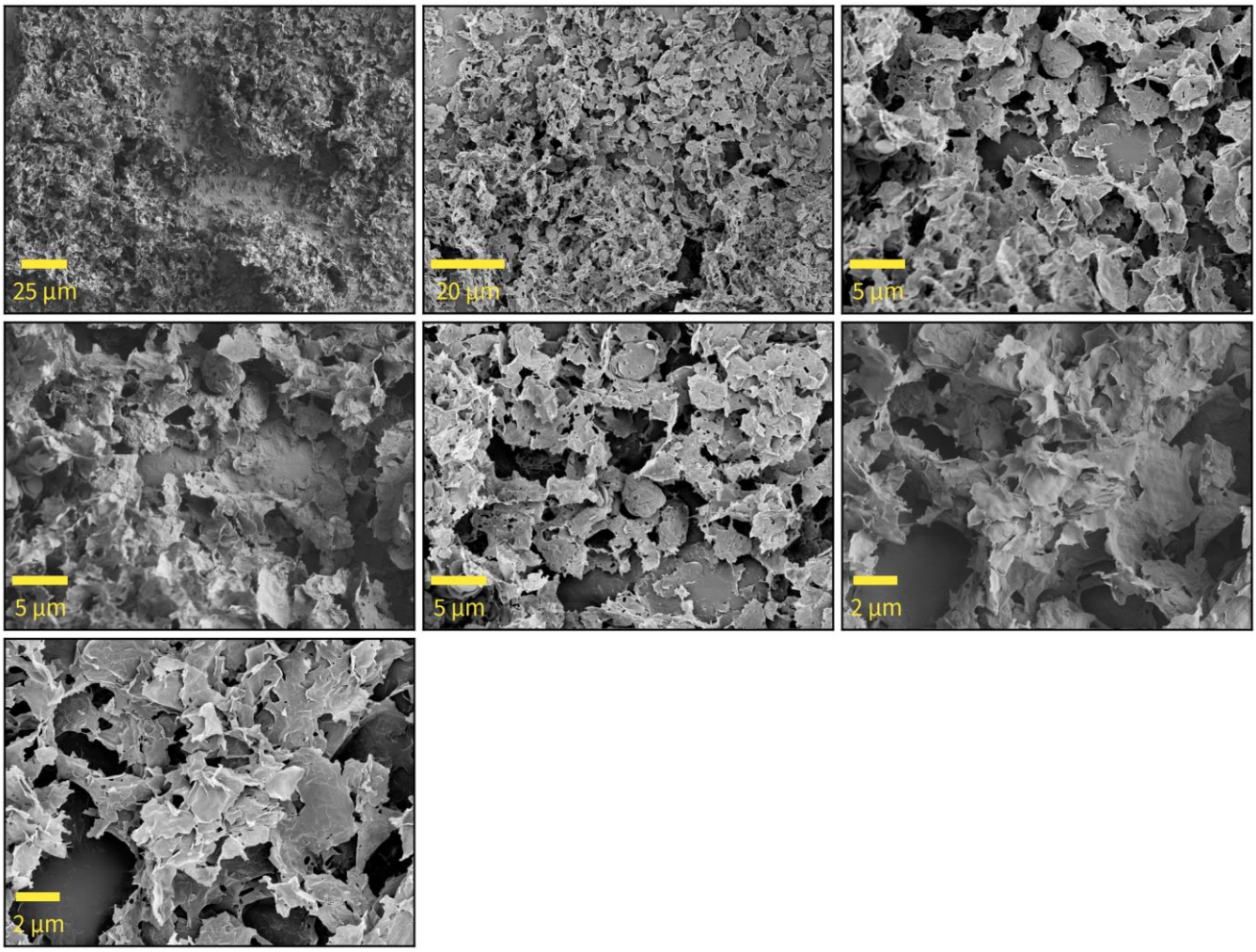

Figure S9. Various magnification SEM images of β-1,3-glucans synthesized at 25 °C.

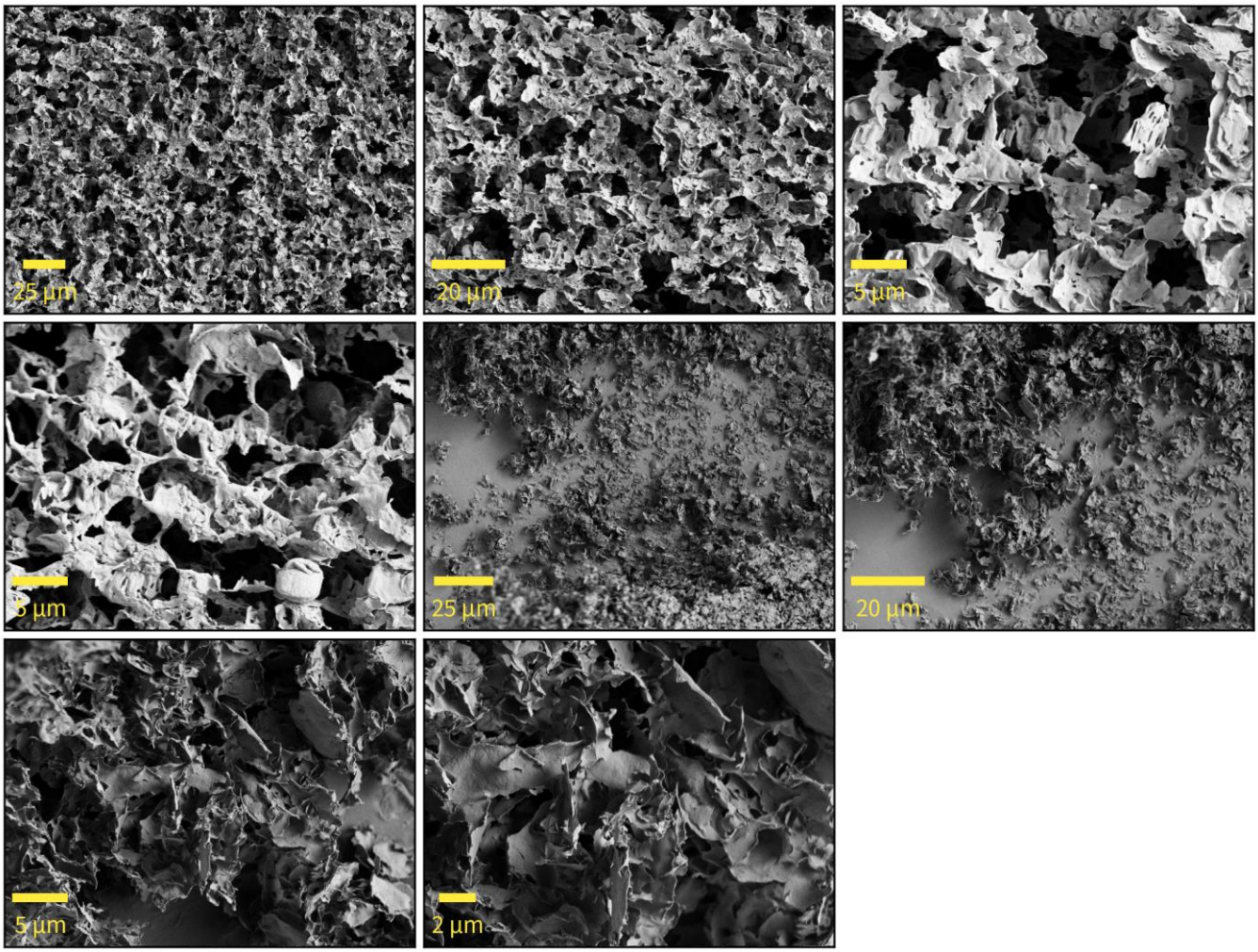

Figure S10. Various magnification SEM images of β-1,3-glucans synthesized at 37 °C.

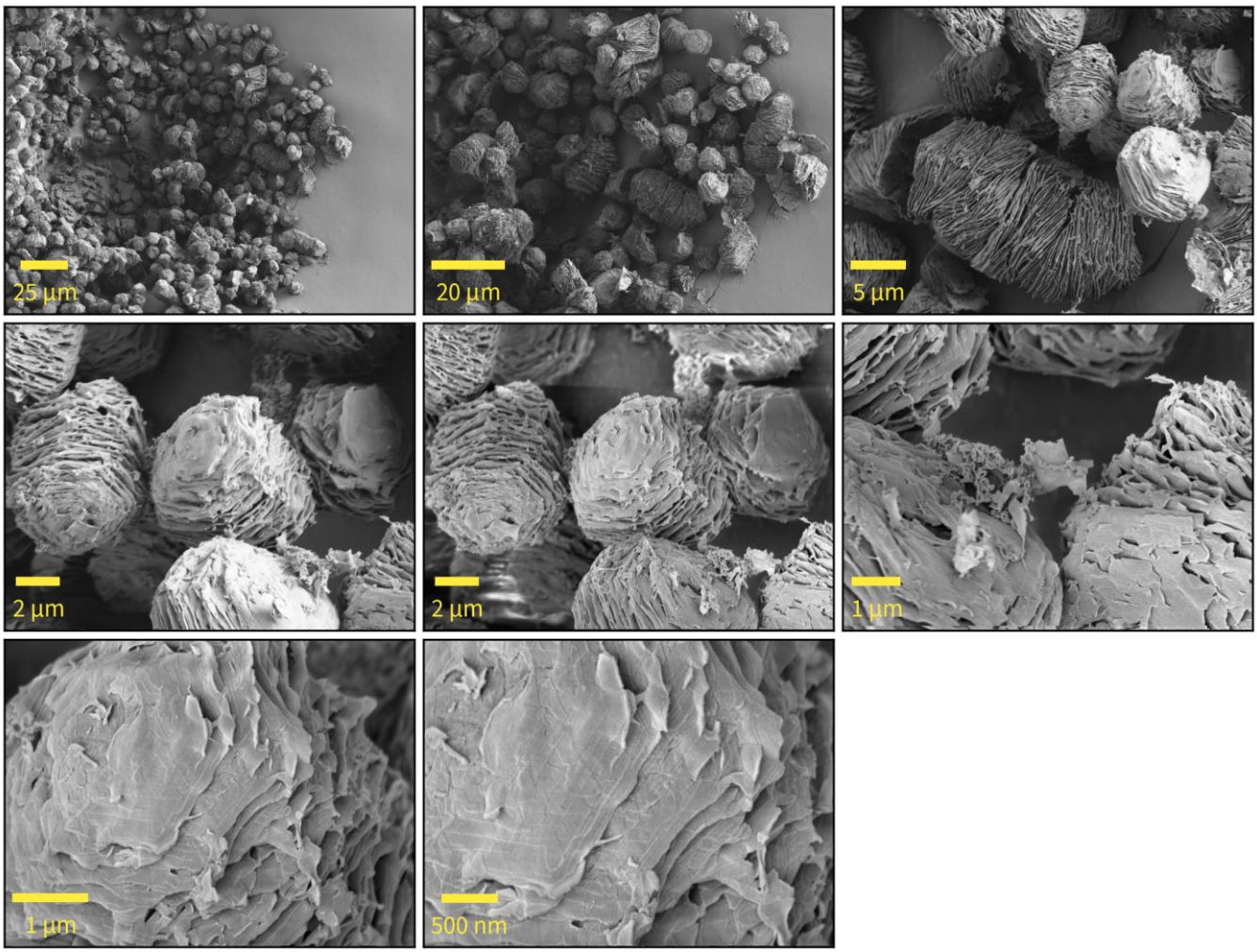

Figure S11. Various magnification SEM images of β-1,3-glucans synthesized at 42 °C.

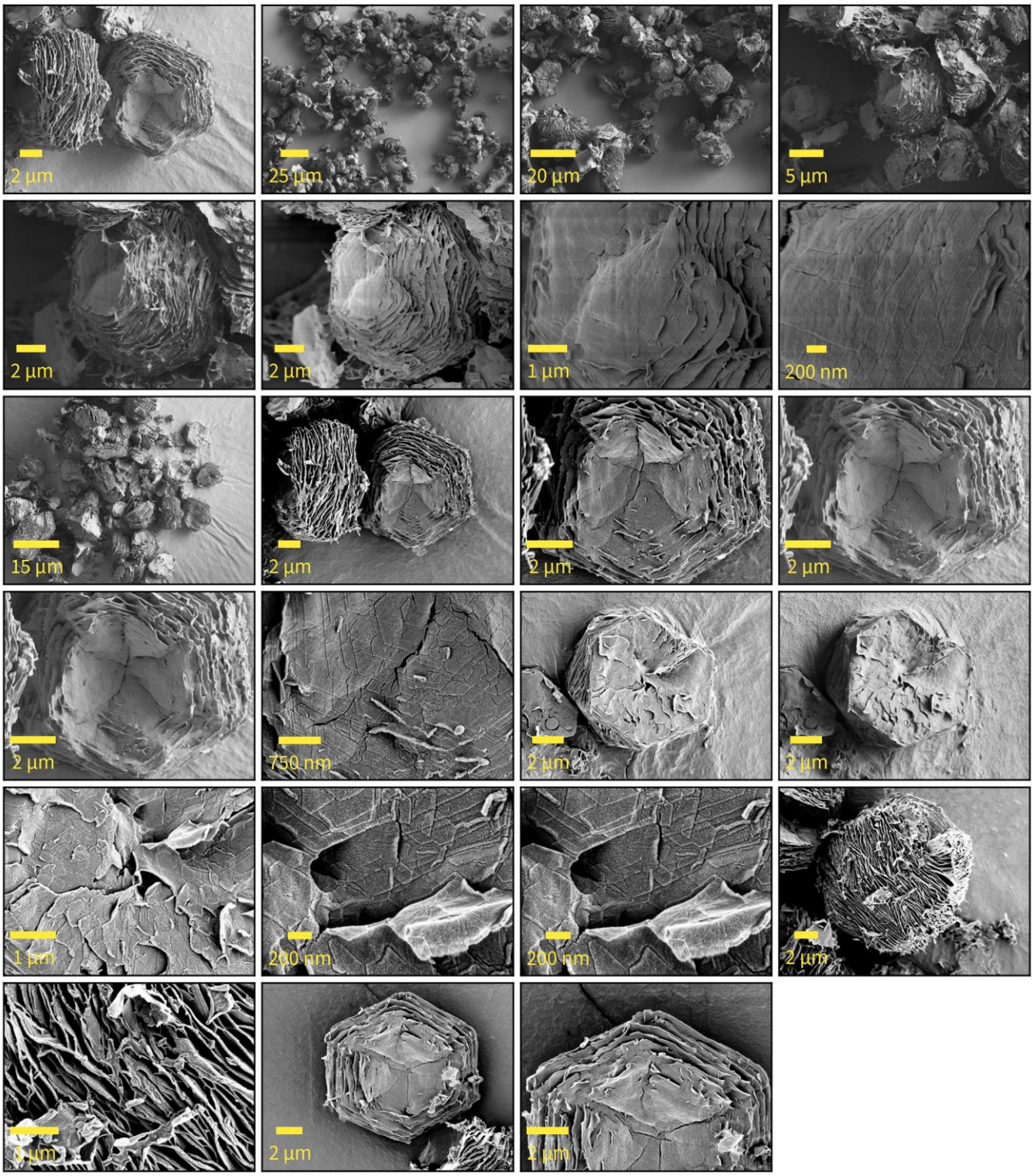

Figure S12. Various magnification SEM images of β-1,3-glucans synthesized at 50 °C.

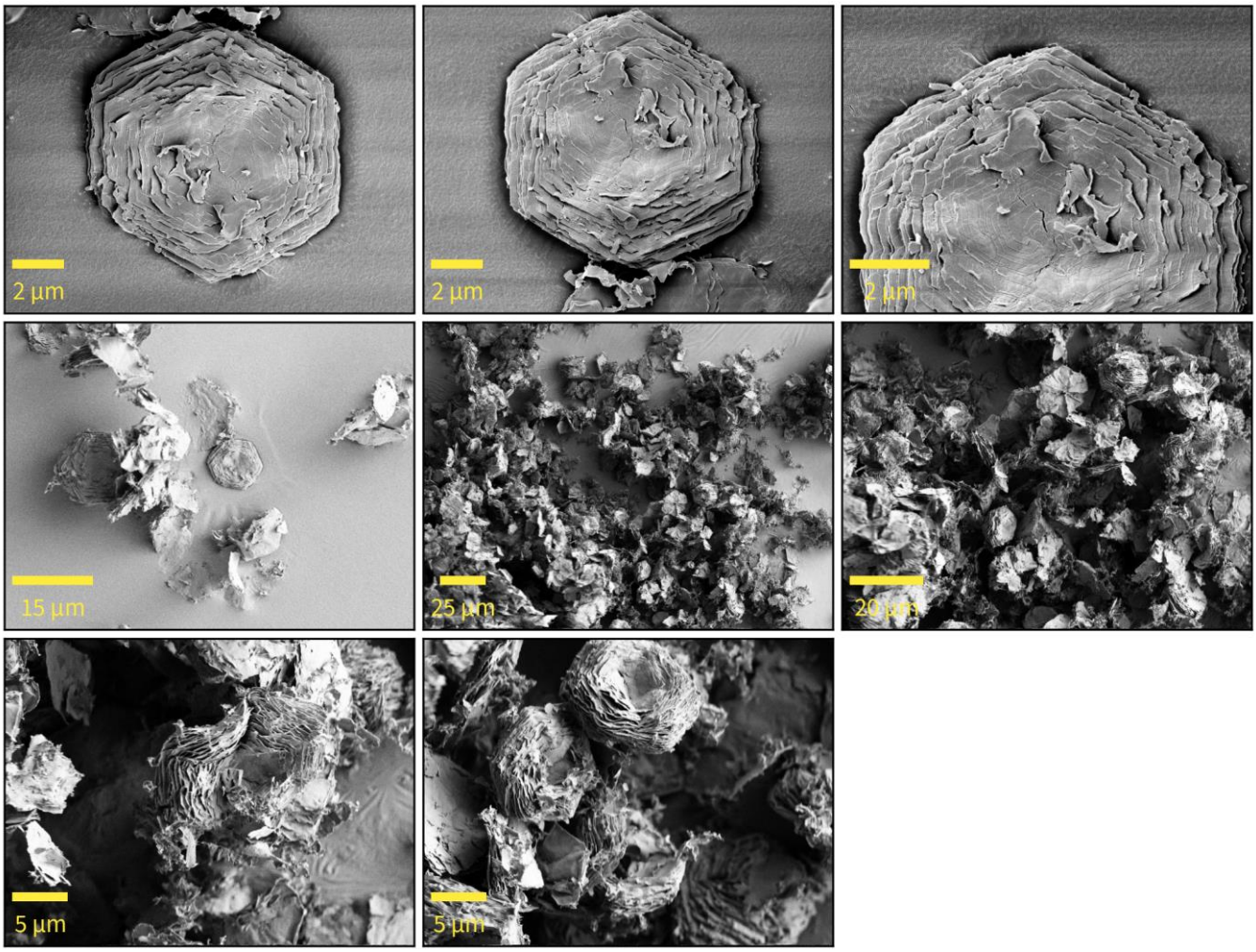

Figure S13. Various magnification SEM images of β-1,3-glucans synthesized at 65 °C.

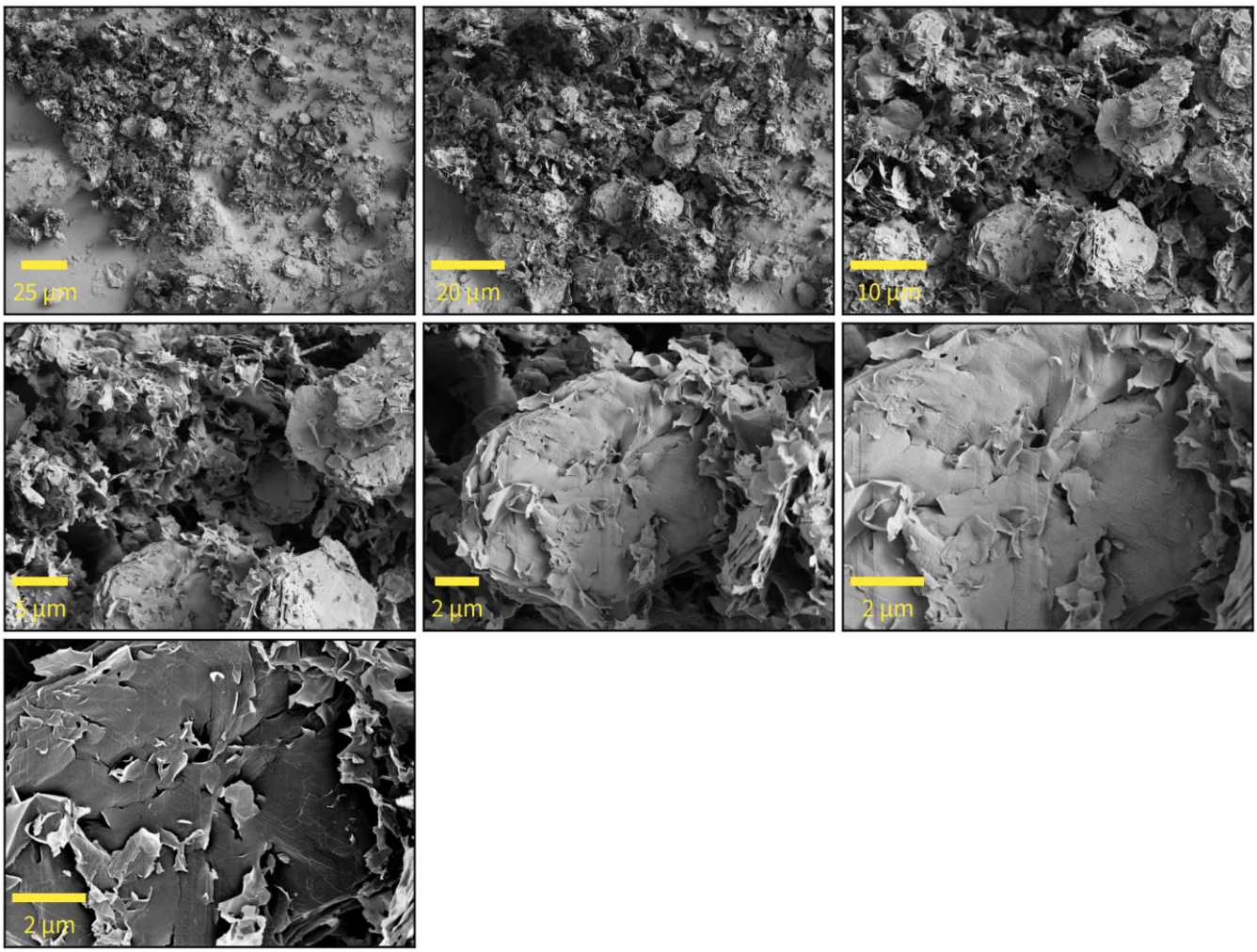

Figure S14. Various magnification SEM images of β-1,3-glucans synthesized at 80 °C.

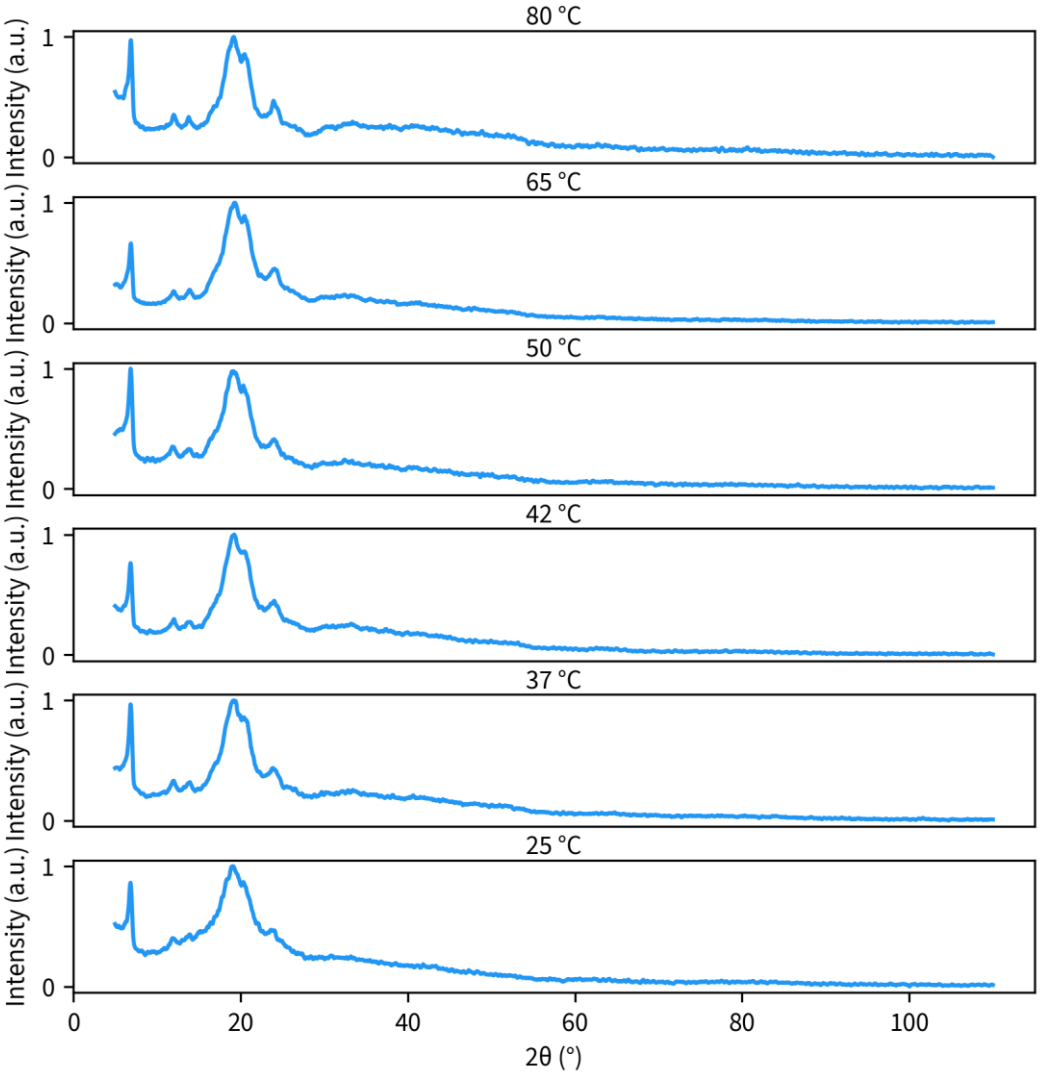

Figure S15. 1D WAXS results without background subtraction for β-1,3-glucans synthesized at various temperatures.

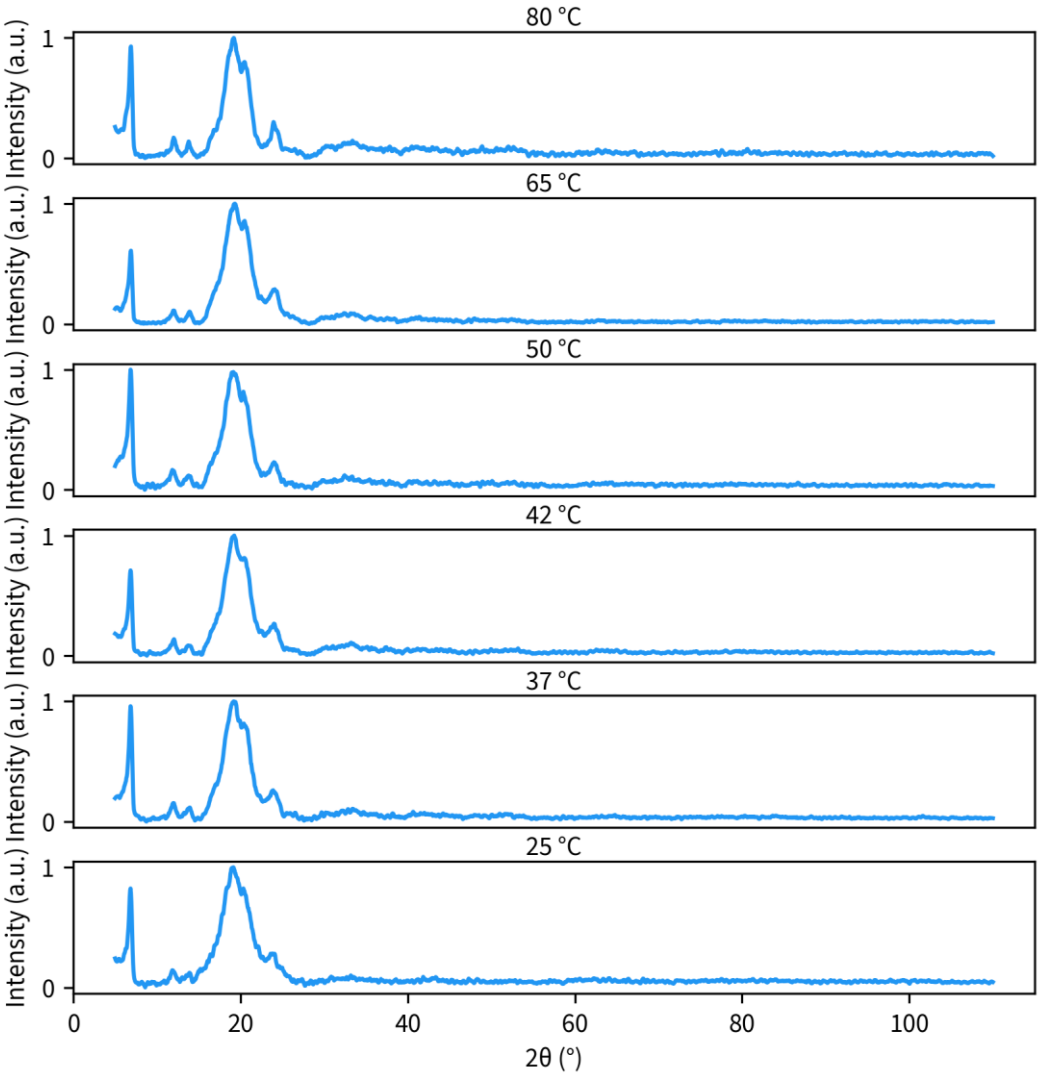

Figure S16. 1D WAXS results with background subtraction for β-1,3-glucans synthesized at various temperatures.

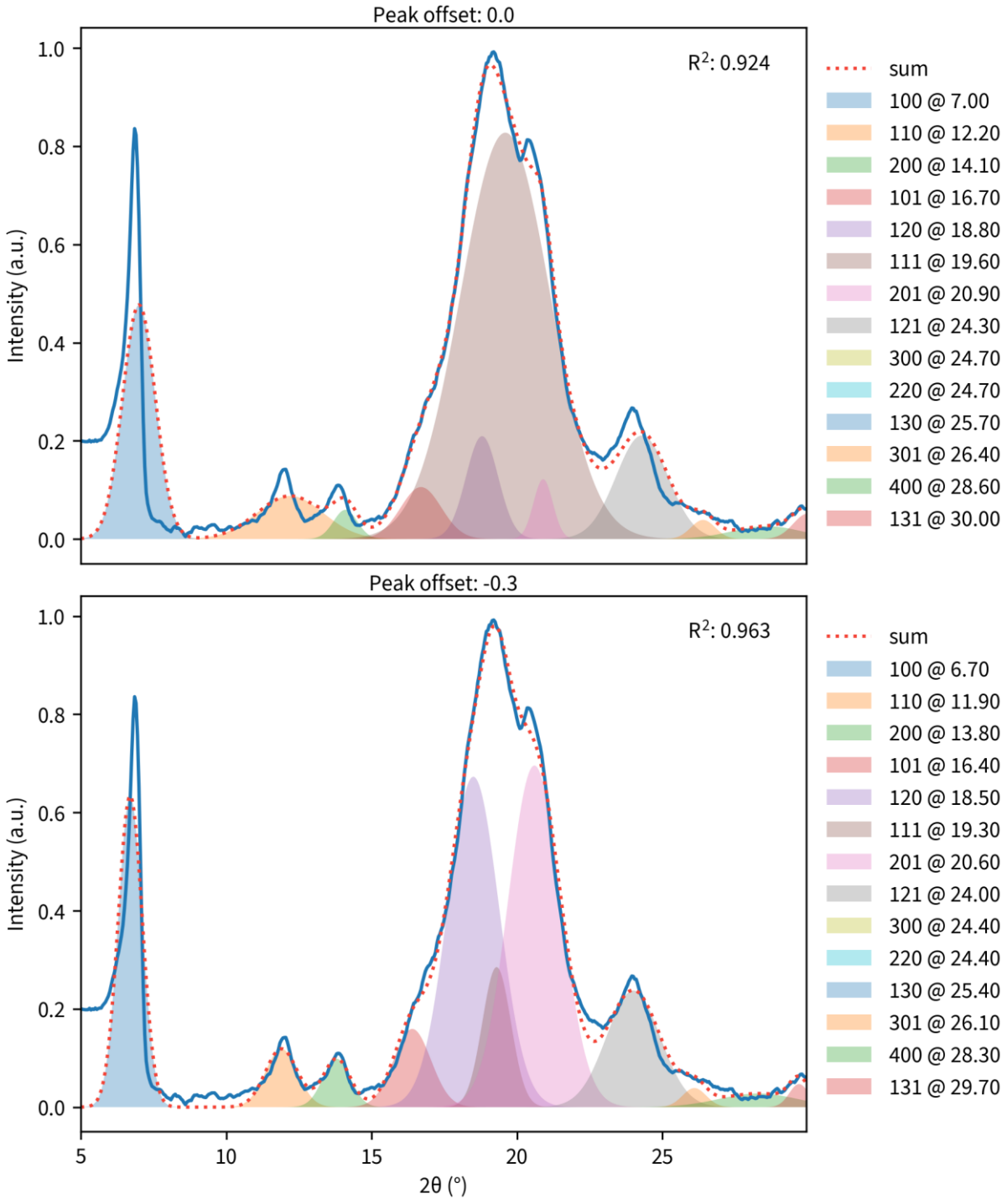

Figure S17. Peak fitting to 1D WAXS data averaged between all measurements. In top panel, peaks are centered as described in literature[19]. In bottom panel, peaks are offset by -0.3 (°), resulting in the best fit. Peak fitting was done using eq. (2).

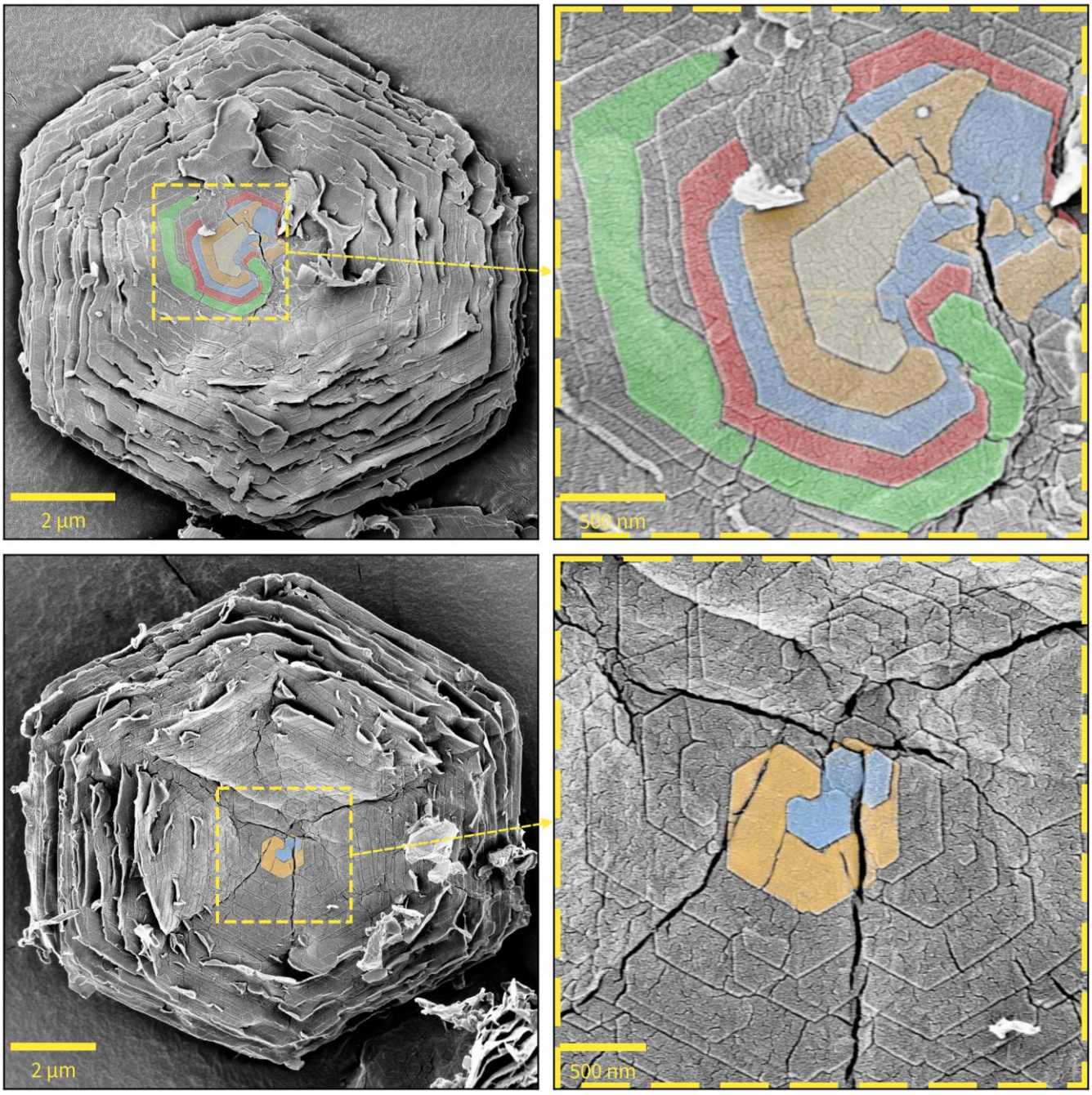

Figure S18. SEM images of nanosheets observed on top layer of hexagonal microparticles. Reaction temperatures were 65 °C for top panel and 50 °C for bottom panel.

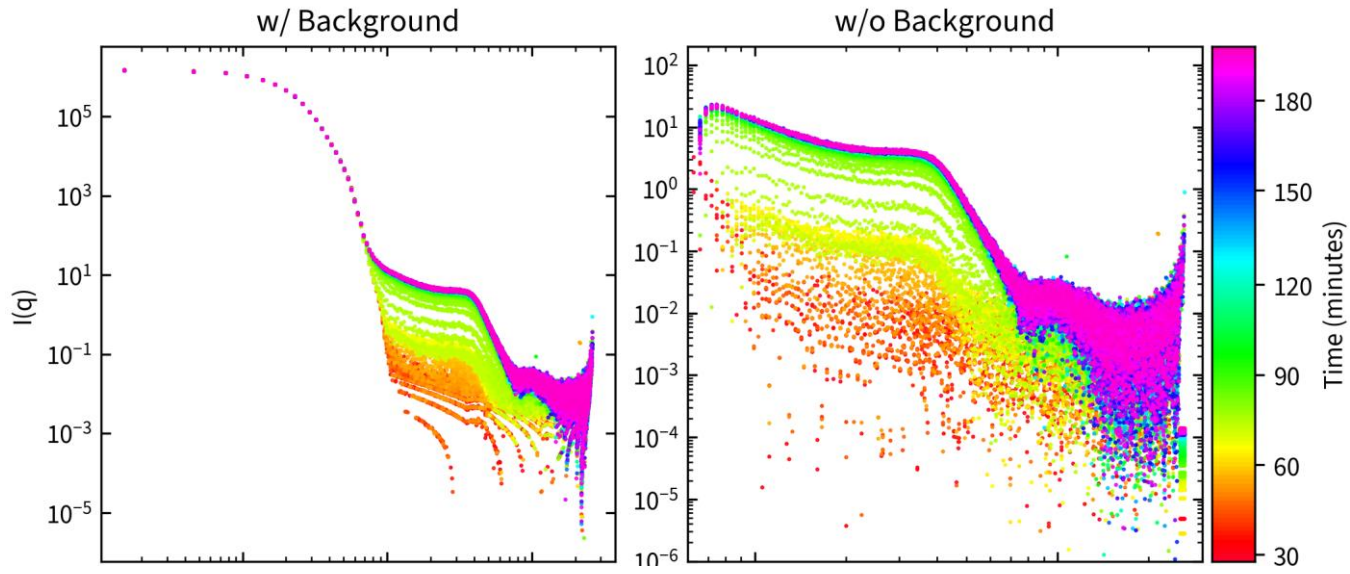

Figure S19. SAXS-data collected during β-1,3-glucan synthesis at 50 °C. Left panel: data without background subtraction, right panel: data with background subtraction. The first five measurements were treated as the background of the measurement.

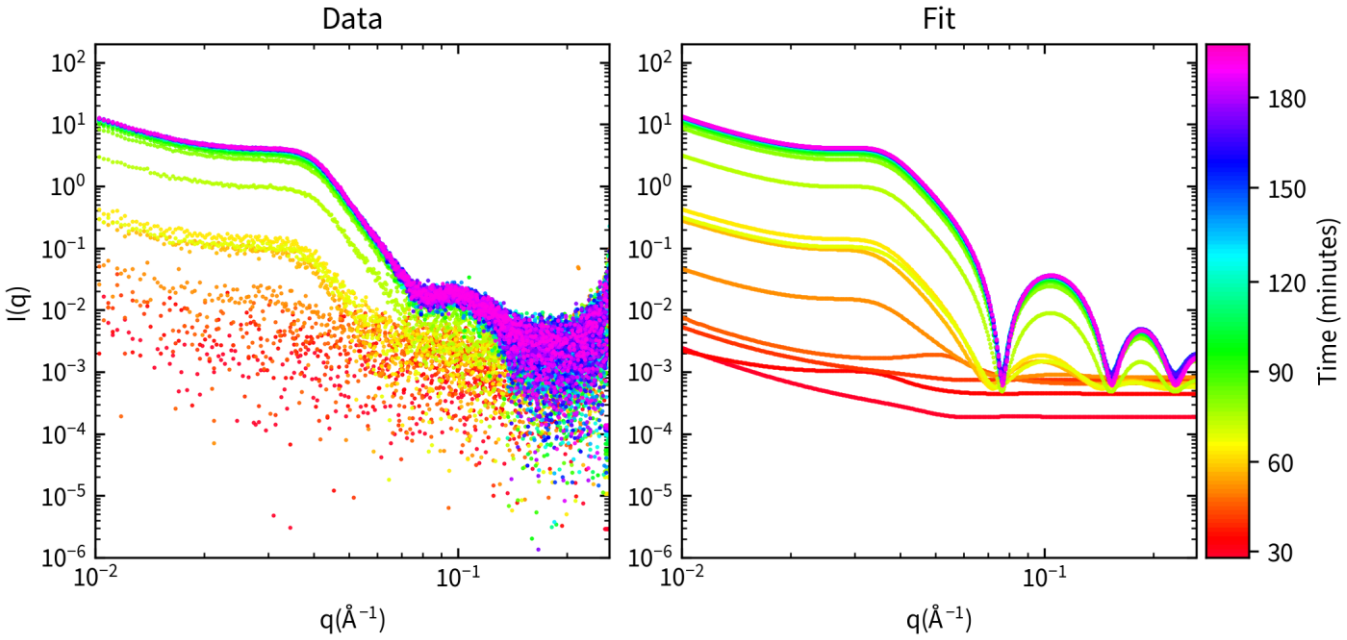

Figure S20. SAXS-data fitting using the model described in literature[4]. Left panel: SAXS-data used for fitting (average of four measurements, 1 minute each), right panel: data generated using the theoretical model with the parameters obtained from the fit.

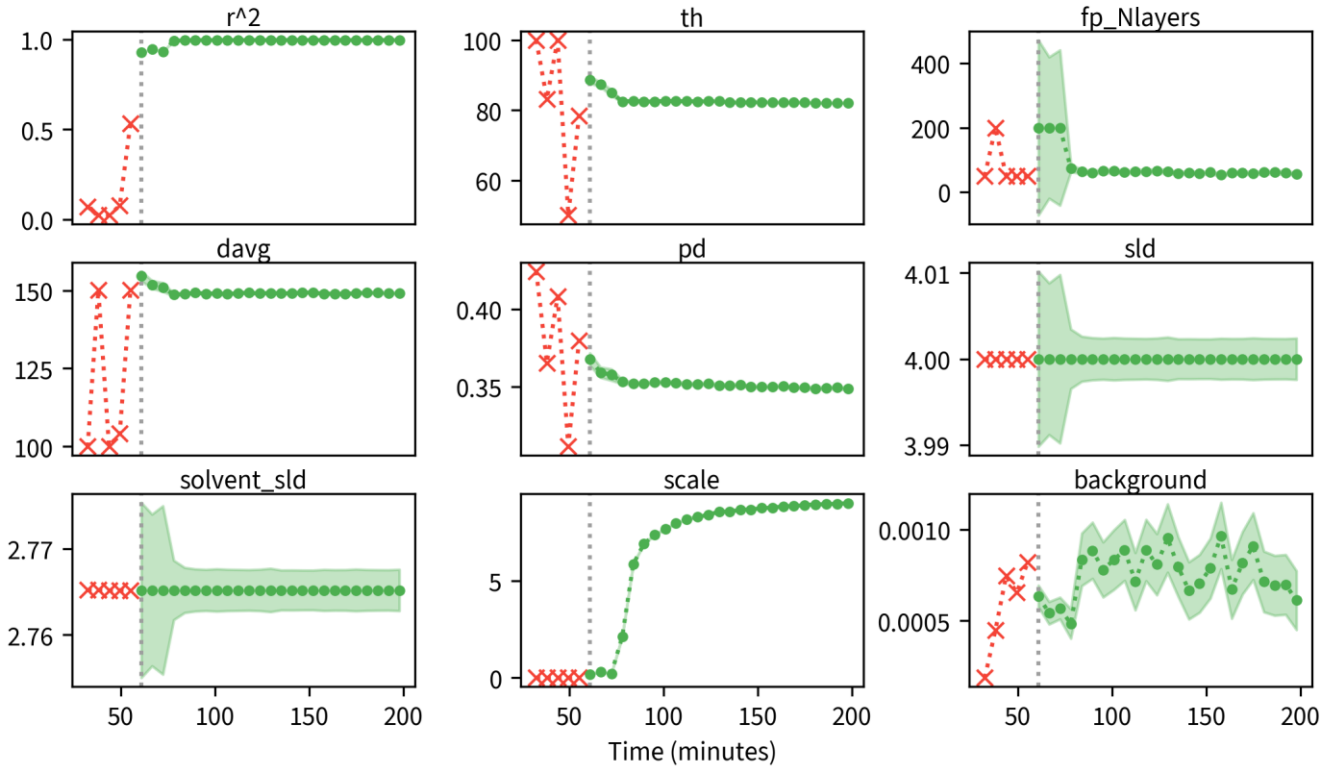

Figure S21. Evolution of parameters of obtained from SAXS-data fitting during β-1,3-glucan synthesis at 50 °C. Red crosses are used to indicate measurement points that could not be fitted well (R^2 < 0.9). Green dots indicate better fit (R^2 > 0.9). One standard deviation errors on parameters estimation are marked with transparent green fill, and are shown for those time points that could be fitted well. Constrains for the fitting are described in the materials and methods section. Abbreviations for each parameter are given on top of each panel, and correspond to r^2: R-squared, the proportion of variance for variables in the model; th: sheet thickness (Å); fp_Nlayers: number of layers; davg: lamellar spacing of paracrystal stack (Å); pd: sigma (polydispersity) of the lamellar spacing (Å); sld: layer scattering length density (10^{-6} Å^{-2}); solvent_sld: solvent scattering length density (10^{-6} Å^{-2}); scale: scale factor or volume fraction; background: source background: cm^{-1}.

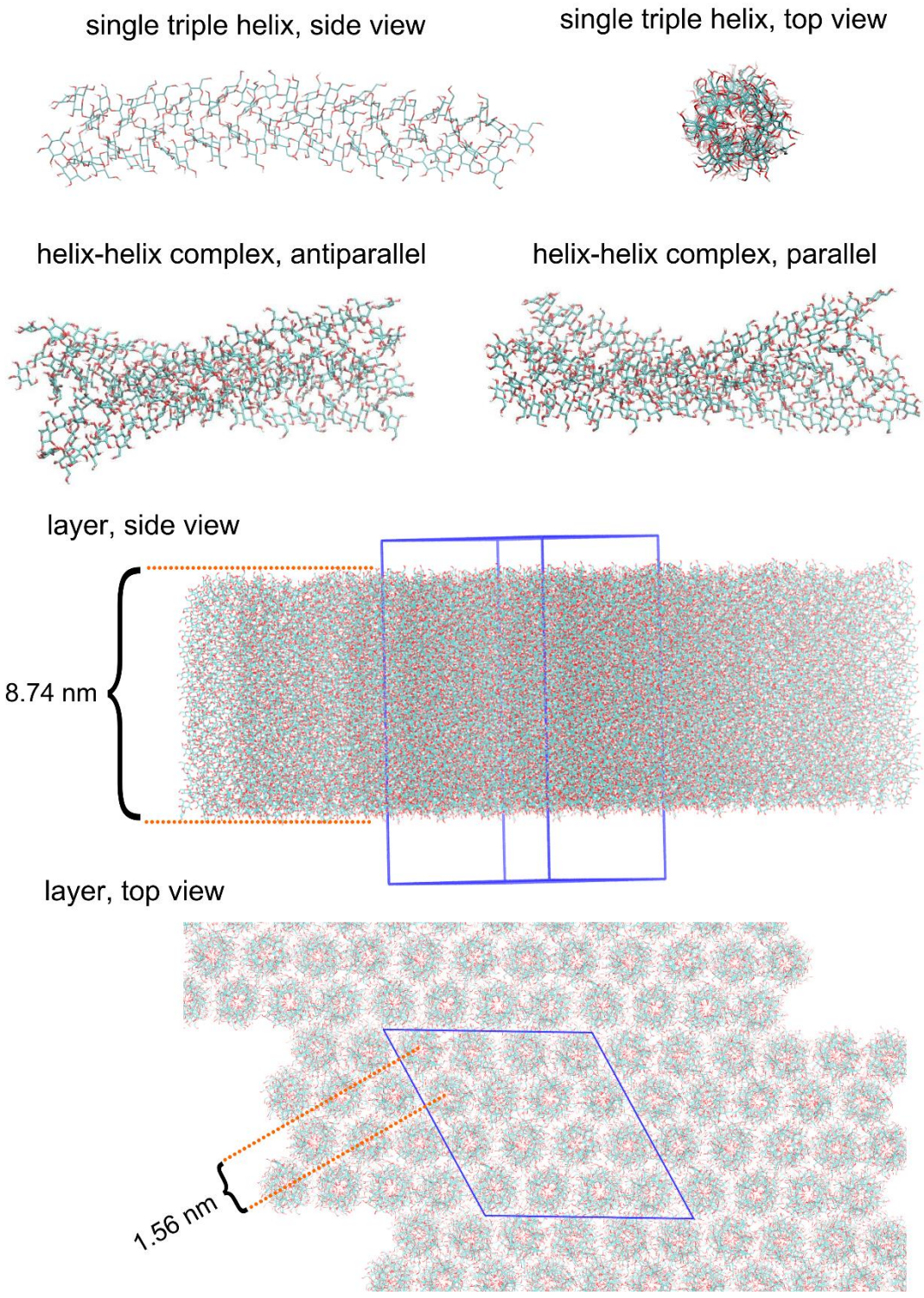

Figure S22. The exemplary snapshots from MD trajectories obtained as a result of simulations carried out for systems (1)-(4). Water molecules are not shown.

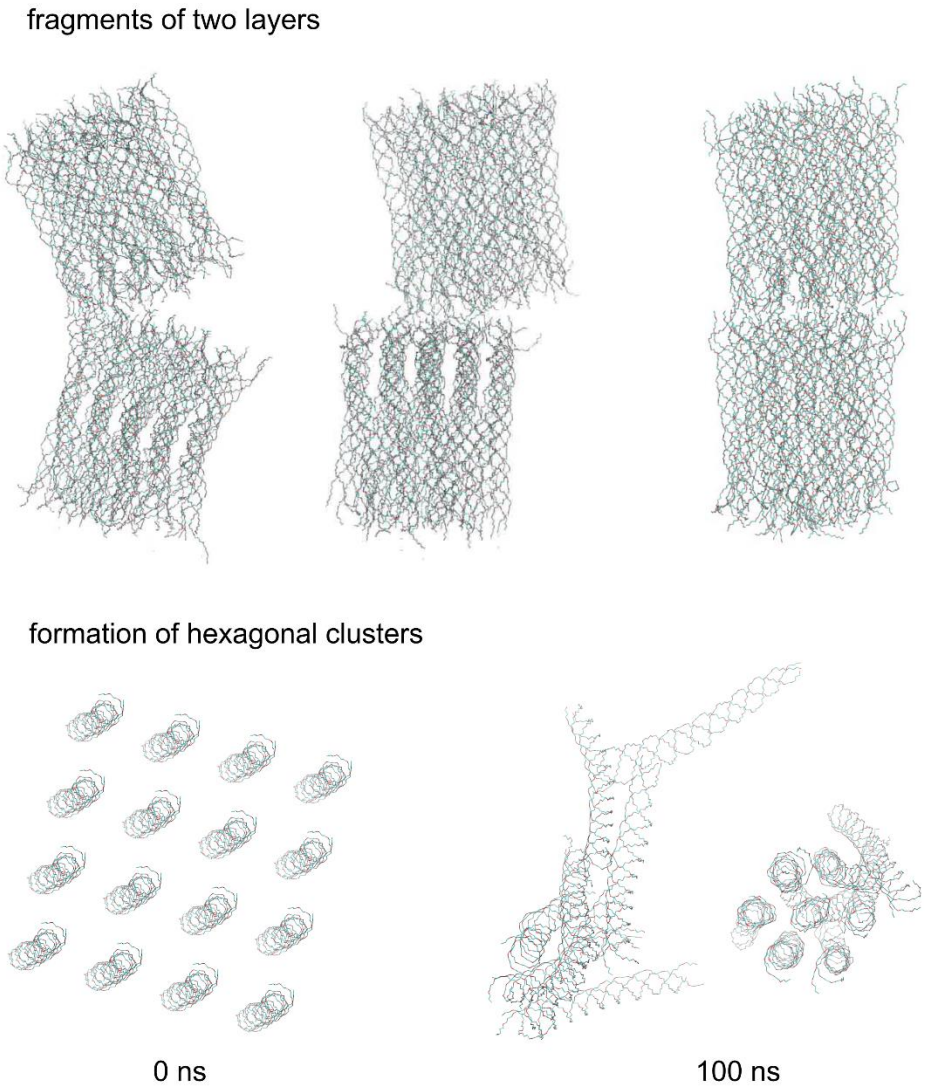

Figure S23. (up) The exemplary snapshots from MD trajectories obtained as a result of triplicated simulations carried out for system (5). (down) The formation of hexagonal cluster composed of seven THs, observed during a simulated annealing MD simulations for system (6). Only backbone atoms in the glucan chain are showed for clarity.

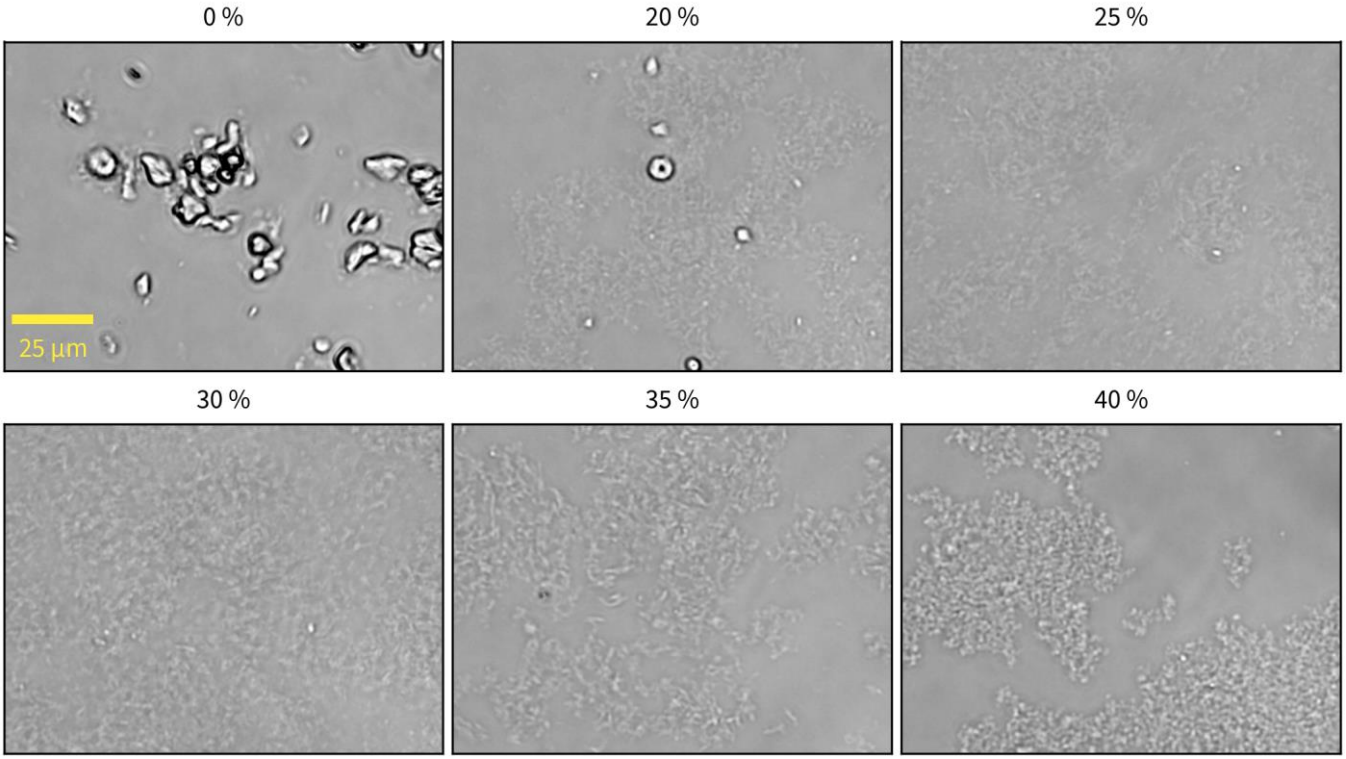

Figure S24. Effect of sonication on hexagonal particle morphology. Sonication was carried out at different amplitudes (0 - 40 %) for 2 minutes. The particles were synthesized at 50 °C and washed in DDIW, followed by sonication and imaging using an optical microscope.

References

[1] D. Gietz, A. St. Jean, R. A. Woods, R. H. Schiestl, *Nucleic Acids Res.* **1992**, *20*, 1425.

[2] D. M. Petrović, I. Kok, A. J. J. Woortman, J. Ćirić, K. Loos, *Anal. Chem.* **2015**, *87*, 9639–9646.

[3] Z. M. Zhang, S. Chen, Y. Z. Liang, *Analyst* **2010**, *135*, 1138–1146.

[4] M. Bergström, J. S. Pedersen, *J. Phys. Chem. B* **1999**, *103*, 8502–8513.

[5] V. Papadopoulou, K. Kosmidis, M. Vlachou, P. Macheras, *Int. J. Pharm.* **2006**, *309*, 44–50.

[6] M. J. Abraham, T. Murtola, R. Schulz, S. Páll, J. C. Smith, B. Hess, E. Lindah, *SoftwareX* **2015**, *1–2*, 19–25.

[7] W. Plazinski, A. Lonardi, P. H. Hünenberger, *J. Comput. Chem.* **2016**, *37*, 354–365.

[8] M. J. Abraham, T. Murtola, R. Schulz, S. Páll, J. C. Smith, B. Hess, E. Lindahl, *SoftwareX* **2015**, *1–2*, 19–25.

[9] G. Bussi, D. Donadio, M. Parrinello, *J. Chem. Phys.* **2007**, *126*.

[10] M. Parrinello, A. Rahman, *J. Appl. Phys.* **1981**, *52*, 7182–7190.

[11] R. W. Hockney, *Methods Comput. Phys. 9 135-211(1970).* **n.d.**

[12] S. Miyamoto, P. A. Kollman, *J. Comput. Chem.* **1992**, *13*, 952–962.

[13] B. Hess, *J. Chem. Theory Comput.* **2008**, *4*, 116–122.

[14] T. N. Heinz, W. F. Van Gunsteren, P. H. Hünenberger, *J. Chem. Phys.* **2001**, *115*, 1125–1136.

[15] S. Kumar, D. Bouzida, R. H. Swendsen, P. A. Kollman, J. M. Rosenberg, *J. Comput. Chem.* **1992**, *13*, 1011–1021.

[16] J. S. Hub, B. L. De Groot, D. Van Der Spoel, *J. Chem. Theory Comput.* **2010**, *6*, 3713–3720.

[17] J. G. Kirkwood, *J. Chem. Phys.* **1935**, *3*, 300–313.

[18] C. H. Bennett, *J. Comput. Phys.* **1976**, *22*, 245–268.

[19] Y. Deslandes, R. H. Marchessault, A. Sarko, *Macromolecules* **1980**, *13*, 1466–1471.